

Can acoustic waves be used to promote collisional growth of cloud droplets?

Lian-Ping Wang and Zhuangzhuang Tian
Department of Mechanics and Aerospace Engineering
Southern University of Science and Technology, China
wanglp@sustech.edu.cn



Acknowledgements: Dr. Jun Qiu, Dr. Wojtek Grabowski

Atmospheric Physics seminar, Institute of Geophysics, University of Warsaw
Friday, November 10, 2023, 13:15-14:15

<https://www.igf.fuw.edu.pl/en/seminars/presentation/can-acoustic-waves-be-used-to-promote-collisional-2023-2024-34fe2f/>

Outline



- **Descriptions of a 1D acoustic wave and its intensity**
- **The Kundt's Tube, acoustic coagulation and its mechanisms**
- **Motivation and objectives**
- **Numerical method to solve the stochastic coalescence equation**
- **Droplet growth under the combined influence of gravity and acoustic waves**
- **Summary**



Part 1

Descriptions of a 1D acoustic wave and its intensity

1D longitudinal **linearized** acoustic wave equation: ideal gas, isentropic flow



No viscous friction, isentropic flow [First assumption]

$$p = \rho RT, \quad T = \frac{p}{\rho R}, \quad dT = \frac{1}{\rho R} dp - \frac{p}{\rho^2 R} d\rho$$

$$ds = \frac{C_v dT}{T} - \frac{R}{\rho} d\rho = \frac{C_v}{p} dp - \frac{C_p}{\rho} d\rho \approx 0 \Rightarrow \frac{p}{p_0} = \left(\frac{\rho}{\rho_0} \right)^\gamma \quad \gamma = \frac{C_p}{C_v}$$

Small density and pressure fluctuations [Second assumption]

$$\frac{p - p_0}{p_0} \ll 1, \quad \frac{\rho - \rho_0}{\rho_0} \ll 1 \Rightarrow \boxed{\frac{dp}{p_0} = \gamma \frac{d\rho}{\rho_0}}$$

Continuity and momentum equations

$$\frac{\partial \rho}{\partial t} + \frac{\partial(\rho u)}{\partial x} = 0 \Rightarrow \text{Linearize} \quad \boxed{\frac{\partial \rho}{\partial t} + \rho_0 \frac{\partial u}{\partial x} = 0}$$

$$\rho \frac{\partial u}{\partial t} + \rho u \frac{\partial u}{\partial x} + \frac{\partial p}{\partial x} = 0 \Rightarrow \text{Linearize} \quad \boxed{\rho_0 \frac{\partial u}{\partial t} + \frac{\partial p}{\partial x} = 0}$$

Eliminate u from the above two

$$\frac{\partial^2 \rho}{\partial t^2} = \frac{\partial^2 p}{\partial x^2} \Rightarrow \frac{\partial^2 \rho}{\partial t^2} = \frac{\gamma p_0}{\rho_0} \frac{\partial^2 \rho}{\partial x^2} = \gamma RT_0 \frac{\partial^2 \rho}{\partial x^2} = c_s^2 \frac{\partial^2 \rho}{\partial x^2}$$

$$\boxed{\frac{\partial^2 \rho}{\partial t^2} - c_s^2 \frac{\partial^2 \rho}{\partial x^2} = 0}$$

$$\boxed{\frac{\partial^2 p}{\partial t^2} - c_s^2 \frac{\partial^2 p}{\partial x^2} = 0}$$

$$\boxed{\frac{\partial^2 u}{\partial t^2} - c_s^2 \frac{\partial^2 u}{\partial x^2} = 0}$$

u, ρ, p satisfy
the same wave equation

The speed of sound
 $c_s = \sqrt{\gamma RT_0}$

General solutions

$$\rho = F_{Left}(x + c_s t) + F_{Right}(x - c_s t)$$

An elemental solution is then

$$\delta p(x, t) = c^2 \delta \rho = p_{rms} \sqrt{2} \cos(kx - kc_s t)$$

$$u = \frac{p_{rms} \sqrt{2}}{\rho_0 c_s} \cos(kx - kc_s t)$$

$$kc_s = 2\pi f$$

p_{rms} = rms sound pressure



1D longitudinal acoustic wave equation: **some terminology**

An elemental solution is then $\delta p(x, t) = c^2 \delta \rho = p_{rms} \sqrt{2} \cos(kx - kc_s t)$

$$u = \frac{p_{rms} \sqrt{2}}{\rho_0 c_s} \cos(kx - kc_s t) = u_0 \cos(kx - kc_s t)$$

u_0
velocity amplitude

The average radiated power intensity ($W \cdot m^{-2}$) is $I = \langle \delta p \cdot u \rangle = \frac{p_{rms}^2}{\rho_0 c_s}, \quad u_0 = \sqrt{\frac{2I}{\rho_0 c_s}}$

The sound pressure level (SPL) in dB

$$SPL = 10 \log_{10} \left(\frac{I}{I_{ref}} \right) = 10 \log_{10} \left(\frac{\delta p_{rms}^2}{\delta p_{rms,ref}^2} \right) = 20 \log_{10} \left(\frac{\delta p_{rms}}{\delta p_{rms,ref}} \right)$$

$$I_{ref} \equiv \frac{(20 \cdot 10^{-6} \text{ Pa})^2}{1.2 \cdot 344} = 0.97 \cdot 10^{-12} \text{ W/m}^2$$

$$c_s = 344 \frac{m}{s}, \quad \rho_0 = 1.2 \frac{kg}{m^3}, \quad p_0 = 101.325 \text{ kPa}, \quad \gamma = 1.4$$



Van Wijhe (2013)

$f = 1000 \text{ Hz}, \text{ time scale} = 0.001 \text{ s}$

	AIR	140dB	150dB	160dB
I	Intensity	97W/m ²	970 W/m ²	9695 W/m ²
p_{rms}	Pressure amplitude (RMS)	200Pa	632Pa	2 000Pa
p_{rms}/p_0	%of atmospheric pressure	0.2%	0.6%	2.0%
u_0	Velocity amplitude	0.69m/s	2.16m/s	6.86m/s
u_0/c_s	% of speed of sound	0.2%	0.6%	2.0%
$s_0 = u_0/(2\pi f)$	Amplitude	0.11 mm	0.34 mm	1.1 mm
$\frac{s_0}{\lambda} = u_0/(2\pi c_s)$	% of wavelength	0.03 %	0.095 %	0.3 %

Extremely low-Ma compressible flow, short time scale, significant velocity

$d_p = 10 \mu\text{m}$ cloud droplets, $\tau_p = 0.0003 \text{ s}$, terminal velocity $W_p = 0.32 \text{ cm/s}$

- Could be effective to produce relative motion for μm -size particles, when $u_0 \gg W_p$
- May need high-frequency to produce significant “inertia” effect: $f\tau_p \sim 1$
- There could be an optimal sound-wave frequency for acoustic coagulation



Part 2

The Kundt's tube, acoustic coagulation and its mechanisms

The Kundt's Tube (1866): A way to measure the sound speed by dust stripes



August Kundt, German Physicist, 1839-1894

August Kundt, 1866. “Ueber eine neue Art akustischer Staubfiguren und über die Anwendung derselben zur Bestimmung der Schallgeschwindigkeit in festen Körpern und Gasen”. *Annalen der Physik*, 203(4), pp.497-523.

“About a new type of acoustic dust figures and about the application of them to determine the speed of sound in solid bodies and gases”

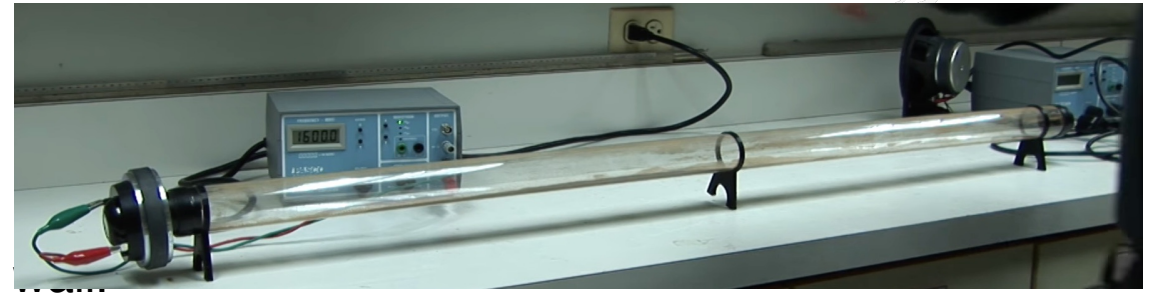


The Kundt's Tube (1866): Longitudinal standing sound waves

Kundt's tube with dust particles, see YouTube video

<https://www.youtube.com/watch?v=Nbhh0B2ajaQ>

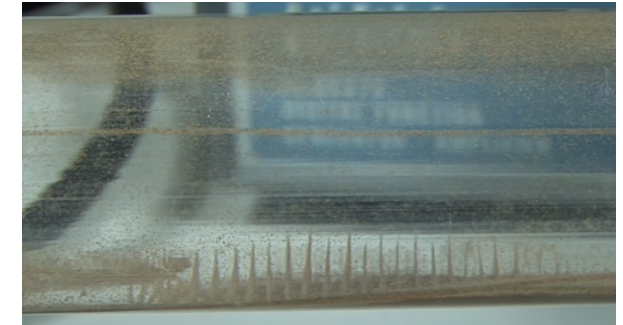
The movable piston at the other end serves as the reflecting



$$\frac{\partial^2 s}{\partial t^2} - \frac{1}{c_s^2} \frac{\partial^2 s}{\partial x^2} = 0, \quad s(x, t) = \text{air particle displacement}$$

The analytical solution (method of separation of variables)

$$s(x = L, t) = a \cdot \frac{\sin \frac{2\pi f x}{c_s}}{\sin \frac{2\pi f L}{c_s}} \cdot \cos(2\pi f t)$$



Positions of nodes (locations of zero displacements): $\frac{2\pi f \delta x}{c_s} = n\pi$, $c_s = 2f\delta x$, $\delta x \sim 10\text{cm}$ in this experiment

c_s = speed of the sound, f = frequency of the sound wave, λ is the wave length of sound waves

The distance between the dust is half $\delta x = 0.5\lambda$

At one end, a loudspeaker attached to a signal generator producing a sine wave.

The other end of the tube is blocked by a movable piston which can be used to adjust the length of the tube.

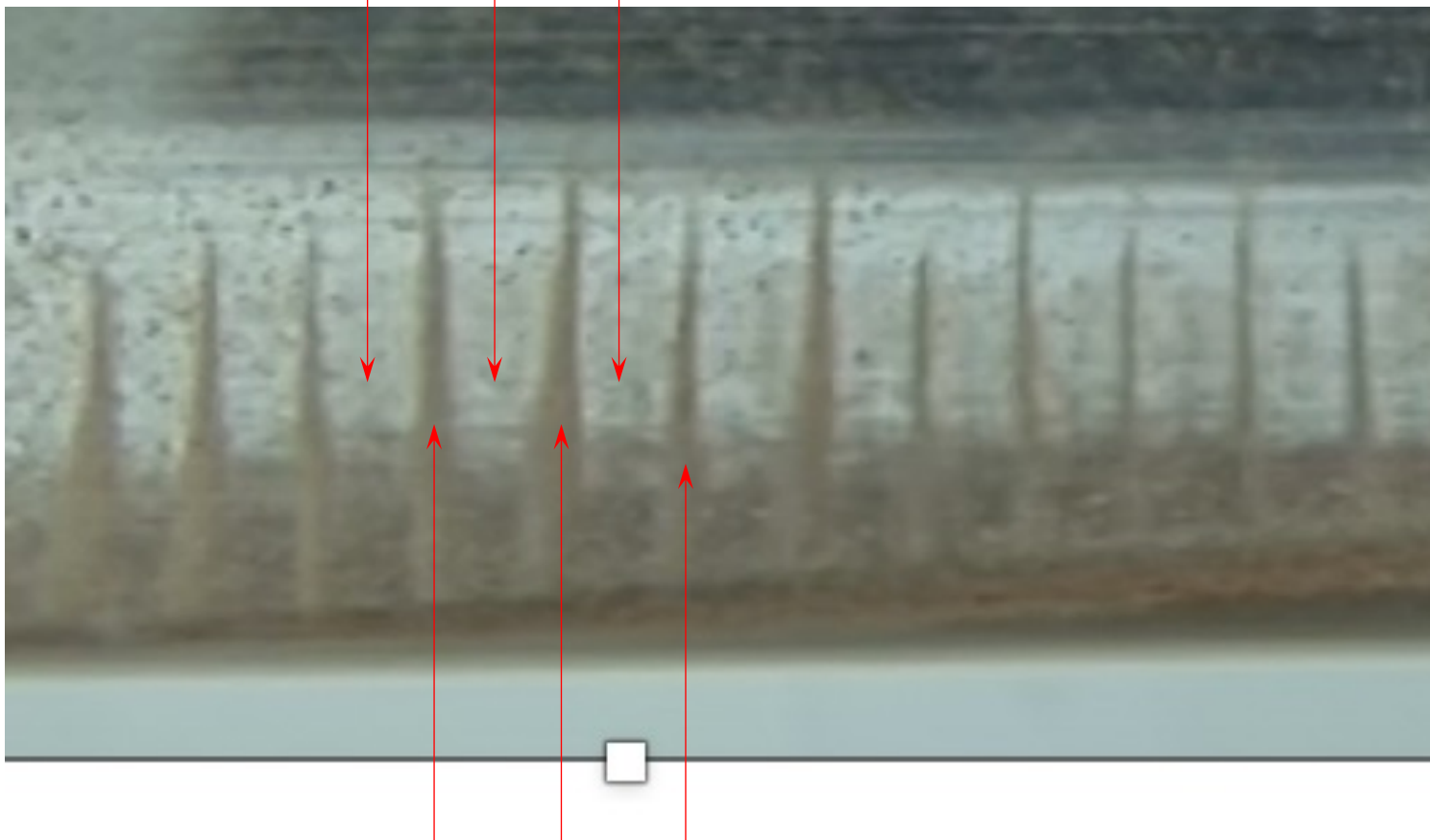
The tube needs to be at resonance. The sound waves in the tube are in the form of standing sound waves.



**YouTube video by Dr. Timothy McCaskey
Department of Science and mathematics
Columbia College Chicago**



anti nodes where air fluid elements displacement is at a maximum



nodes where air fluid elements displacement is zero
(These are pressure **anti-nodes**)

The powder is caught up in the moving air and settles in little piles or lines at these nodes, because the air is still and quiet there. The distance between the piles is one half wavelength $\lambda/2$ of the sound. By measuring the distance between the piles, the wavelength λ of the sound in air can be found. If the frequency f of the sound is known, multiplying it by the wavelength gives the speed of sound c in air.

$$c_s = 2 \times f \times \delta x_{\text{dust layers}}$$

Air density, velocity, and pressure distribution in the Kundt's Tube: one-dimensional model



$$\delta\rho(x, t) = \rho(x, t) - \rho_0 = -\rho_0 \frac{\partial s}{\partial x} = \rho_0 a \cdot \frac{2\pi f}{c_s} \cdot \frac{\cos \frac{2\pi f x}{c_s}}{\sin \frac{2\pi f L}{c_s}} \cdot \cos(2\pi f t)$$

The pressure change is determined by the isentropic relation of an ideal gas

$$\frac{p}{\rho^\gamma} = \text{constant} \quad \rightarrow \quad \delta p = c_s^2 \delta \rho = \delta p_{max} \cdot \cos \frac{2\pi f x}{c_s} \cdot \cos(2\pi f t), \text{ where } \delta p_{max} = a \rho_0 \cdot \frac{2\pi f c_s}{\sin \frac{2\pi f L}{c_s}}$$

The air velocity is

$$u = \frac{\partial s(x, t)}{\partial t} = -2\pi f a \cdot \frac{\sin \frac{2\pi f x}{c_s}}{\sin \frac{2\pi f L}{c_s}} \cdot \sin(2\pi f t) = -\frac{\delta p_{max}}{\rho_0 c_s} \cdot \sin \frac{2\pi f x}{c_s} \cdot \sin(2\pi f t)$$

$$\text{Or: } u = \frac{u_0}{2} \left[\cos \left(\frac{2\pi f x}{c_s} (x + c_s t) \right) - \cos \left(\frac{2\pi f x}{c_s} (x - c_s t) \right) \right]$$

Average intensity of the sound wave

$$I = \langle |\delta p \cdot u| \rangle = \frac{(\delta p_{max})^2}{16\rho_0 c_s}, \quad u_{max} = \frac{\delta p_{max}}{\rho_0 c_s} = \sqrt{\frac{16I}{\rho_0 c_s}}$$

Horizontal movement of a dust particle in standing sound waves

$$u = -u_{max} \cdot \sin \frac{2\pi f x}{c_s} \cdot \sin(2\pi f t), \quad u_{max} = \frac{\delta p_{max}}{\rho_0 c_s}$$

$$\frac{dV}{dt} = \frac{u(Y(t), t) - V}{\tau_p}, \quad \frac{dY}{dt} = V(t)$$

$$u = \frac{u_0}{2} \operatorname{Re} \left[\exp \left(i \frac{2\pi f}{c_s} (x + c_s t) \right) - \exp \left(i \frac{2\pi f}{c_s} (x - c_s t) \right) \right]$$

$$V(t) \approx \frac{u_0}{2} \operatorname{Re} \left\{ \frac{1}{(1 + i \cdot St)} \exp \left(i \frac{2\pi f}{c_s} (x + c_s t) \right) - \frac{1}{(1 - i \cdot St)} \exp \left(i \frac{2\pi f}{c_s} (x - c_s t) \right) \right\}$$

$$V(t) \approx \frac{1}{\sqrt{1 + St^2}} \frac{u_0}{2} \operatorname{Re} \left\{ \exp(i\phi_+) \exp \left(i \frac{2\pi f x}{c_s} (x + c_s t) \right) - \exp(i\phi_-) \exp \left(i \frac{2\pi f}{c_s} (x - c_s t) \right) \right\}$$

amplitude reduction
(e.g., entrainment ratio)

phase shifts

Typical assumptions:

- (1) $u_0 \ll c_s$, slow migration
- (2) $d_p \ll \lambda$, Stokes drag law
- (3) $\rho_p \gg \rho_f$, simplified eqn of motion

Measure of particle inertia effect

$$St = \omega \tau_p = 2\pi f \tau_p$$

Velocity of dust particles of different sizes

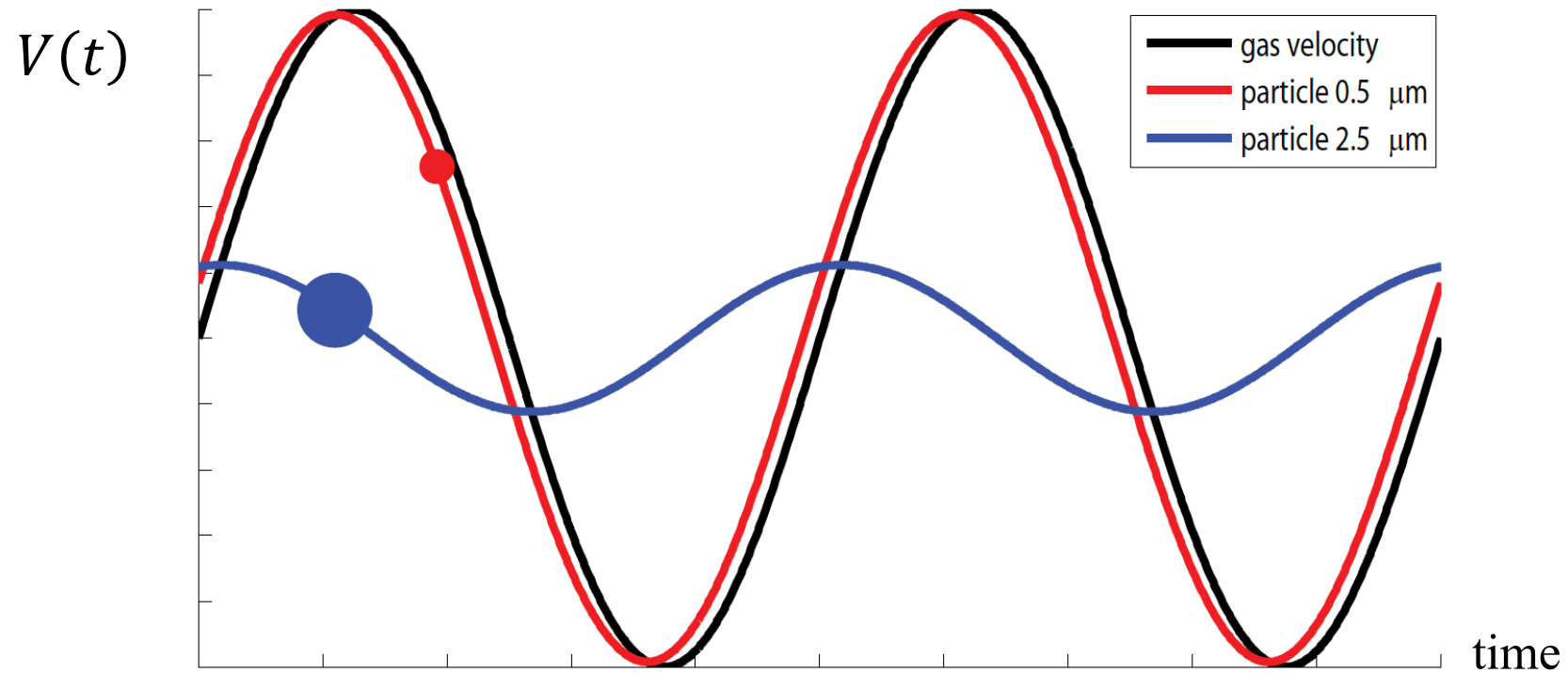


Figure 2-2: Difference of entrainment ratio for two particles of a different size.

Question: can we simulate these dust figures in The Kundt's Tube?



Wall-bounded low-speed compressible flow
Lagrangian tracking of particles



Relative motion between two dust particles: **The orthokinetic particle interaction**

Particles of different sizes will have different amplitude reductions / phase shifts, creating relative motion between large and small particles

$$V_1(t) - V_2(t) \approx \frac{u_0}{2} \operatorname{Re} \left\{ \left[\frac{1}{(1 + i \cdot St_1)} - \frac{1}{(1 + i \cdot St_2)} \right] \exp \left(i \frac{2\pi f}{c_s} (x + c_s t) \right) - \left[\frac{1}{(1 - i \cdot St_1)} - \frac{1}{(1 - i \cdot St_2)} \right] \exp \left(i \frac{2\pi f}{c_s} (x - c_s t) \right) \right\}$$

$$V_1(t) - V_2(t) \approx \frac{|St_1 - St_2|}{\sqrt{(1 + St_1^2)(1 + St_2^2)}} \frac{u_0}{2} \operatorname{Re} \left\{ \exp(i\phi_{12+}) \exp \left(i \frac{2\pi f}{c_s} (x + c_s t) \right) - \exp(i\phi_{12-}) \exp \left(i \frac{2\pi f}{c_s} (x - c_s t) \right) \right\}$$

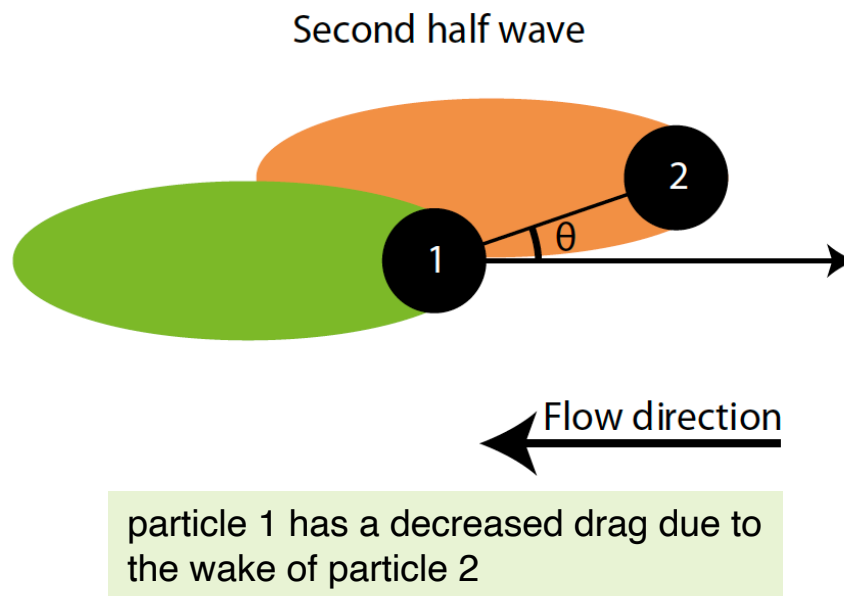
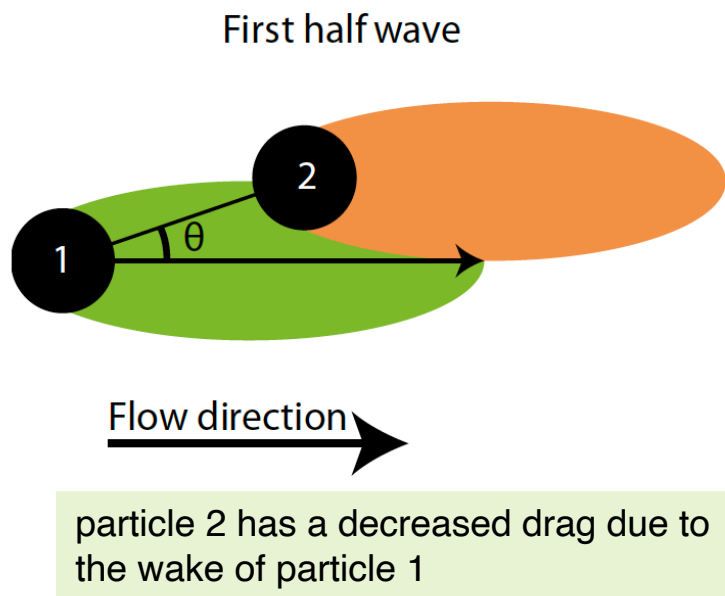
$$\frac{|St_1 - St_2|}{\sqrt{(1 + St_1^2)(1 + St_2^2)}} \text{ obtains a maximum value when } \omega^2 = \frac{-(\tau_{p1}^2 + \tau_{p2}^2) + \sqrt{\tau_{p1}^4 + \tau_{p2}^4 + 14\tau_{p1}^2 \tau_{p2}^2}}{6\tau_{p1}^2 \tau_{p2}^2}$$

Given the sizes of the small and the large particles, an optimum frequency exists (Shaw, 1978).



The relative motion due to the acoustic wake effect

the reduction of distance between two particles due to the mutual slipstreaming in an oscillating flow



Van Wijhe (2013)

Based on the Oseen disturbance flow

$$|V_1(t) - V_2(t)| = \frac{3}{4} \frac{u_0}{\pi r} (d_{p1} l_1 + d_{p2} l_2)$$

r is distance between the two particles

$$l_i = \frac{\mu_i}{\sqrt{1 + 2h_i \mu_i^2 + h_i^2 \mu_i^4}}, \quad h_i = \frac{\rho_g}{\rho_p} \frac{9u_0}{\pi \omega d_{pi}}, \quad \mu_i = \frac{\omega \tau_{pi}}{\sqrt{1 + (\omega \tau_{pi}^2)^2}}$$

The slip coefficient

The Stokes slip coefficient

Andrade, E.D.C., 1936. The coagulation of smoke by supersonic vibrations. Transactions of the Faraday Society, 32, pp.1111-1115.

Hoffmann, T.L., 1997. An extended kernel for acoustic agglomeration simulation based on the acoustic wake effect. J. Aerosol Sci., 28(6), pp.919-936.

Dianov, D. V., Podolski, A. A., & Turubarov, V. I. (1968). Calculation of the hydrodynamic interaction of aerosol particles in a sound field under Oseen flow conditions. Soviet Physics Acoustics-USSR, 13, 314.



Various applications of acoustic coagulation of aerosol particles

Acoustic coagulation was first noted in 1920's

C. Andrade and S.K. Lewer, New Phenomena in a sounding dust tube. Nature, 1929. 124: P. 724-725.

Acoustic coagulation using powerful sirens, to clear airstrip runways from fog

E.P. Mednikov, Acoustic Coagulation and precipitation of aerosols, 1965.

Acoustic coagulation to promote formation of dust agglomerates, for better dust filtration / removal

Scott, 1975, J. Sound Vibration; Somers et al., 1991, J. Aerosol Sci.

How about as a method for cloud seeding / rain enhancement?



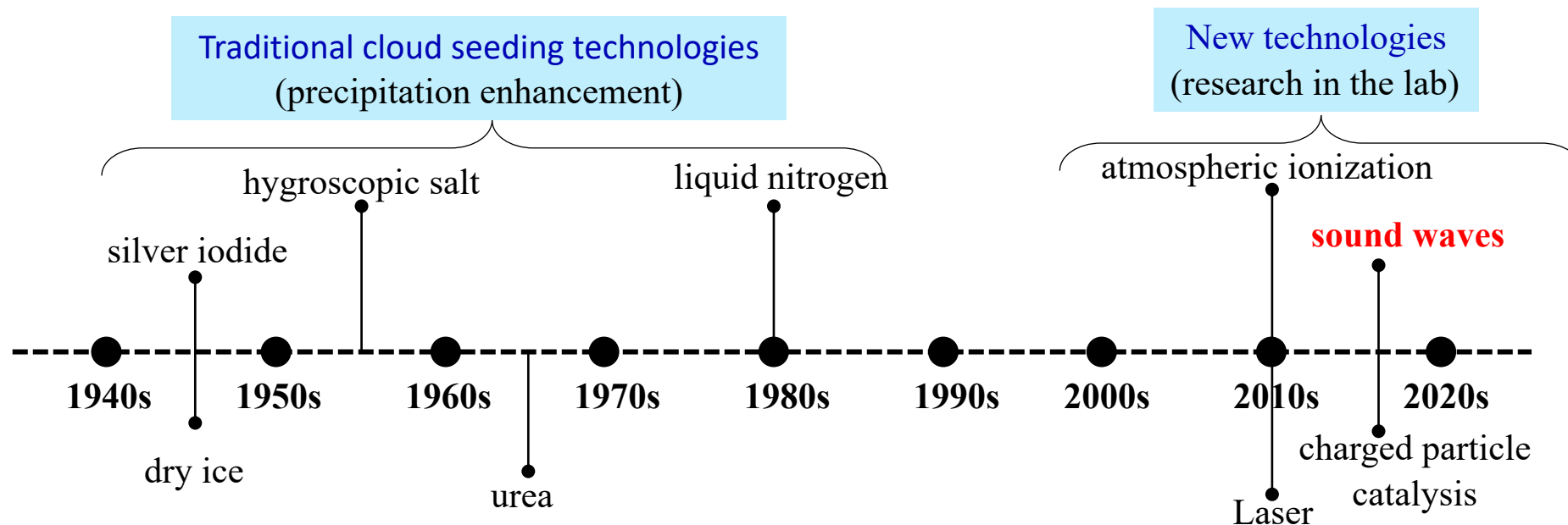
Part 3

Motivation and specific objectives



Artificial Cloud Seeding / Rain Enhancement Technology

- ❑ Major challenges: Weather / Climate changes and lack of fresh water
- ❑ Water resources important for the social and economic development of China, can we explore unconventional water resources?
- ❑ The amount of water in the atmosphere over China $\sim 2.2 \times 10^{16}$ kg (22 trillion tons), 4 times of annual precipitation
- ❑ Precipitation efficiency $\sim 28\%$, a lot of potential to explore atmospheric water resources
- ❑ Sound-wave artificial precipitation: low cost, no catalyst, precise control,



- Sound waves:
- orthokinetic
 - acoustic wakes
 - radiation pressure

Henin, S., et al. (2011). Nature Communications

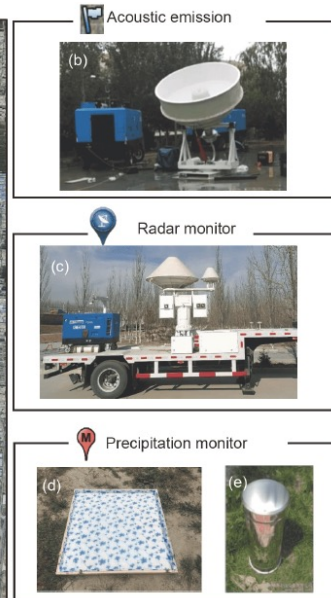
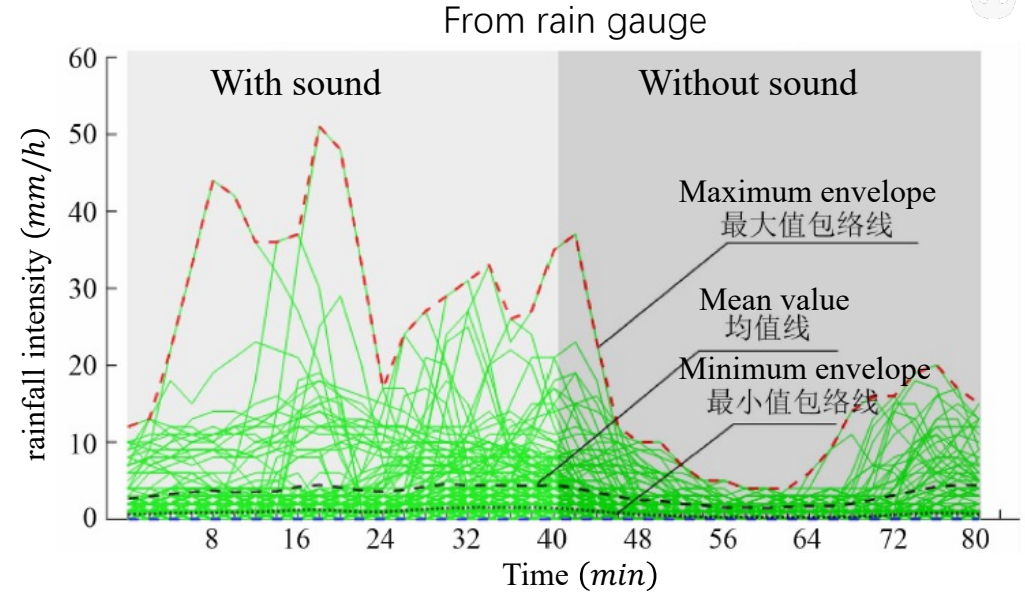
Ju, J. J., et al. (2017). Scientific Reports

Leisner, T., et al. (2013). Proceedings of the National Academy of Sciences

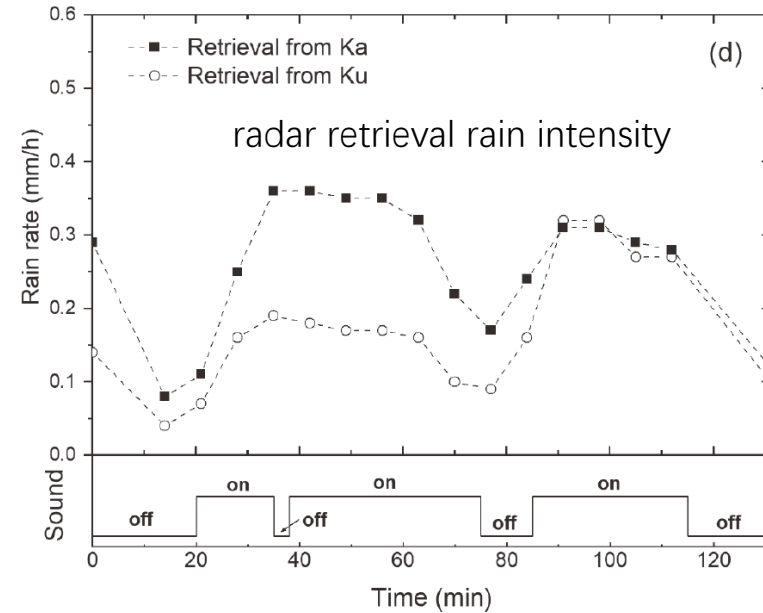
Background: Acoustic agglomeration for rain enhancement – field experiment



Qiu J., et.al.
2020
Tsinghua U.



Wei J.H., et.al.
2021
Qinghai U.



Cloud response to YunZhuFeng field experiment—— “Sky window”



20170811, YunZhuFeng, Kunlun Mountain

Motivation: field and lab experiments on acoustic rain enhancement

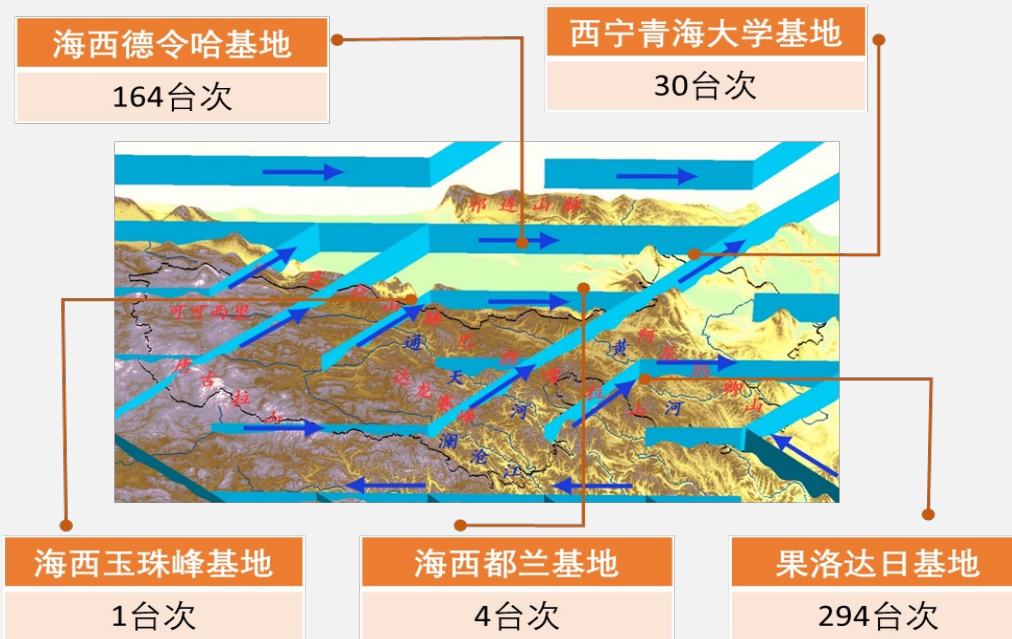


Dr. Jun Qiu, Associate Research Professor in Department of Hydraulic Engineering at Tsinghua U.



- Hydraulic Engineering: fresh water resources
- NSFC projects: “Study of acoustic coagulation mechanisms of cloud droplet” “Theory and techniques to develop and control water resources for the Southwest River region”
- Achieved some initial success (10~17%, 2021-Sci China-Tech Sciences) to promote precipitation using sound waves, and recently built an acoustic cloud chamber with the goal to better understand the interactions of sound wave, air turbulence, and precipitation

作业气象条件	
云	低云
	高云
	厚云
	薄云
雨	小雨
	中雨
	大雨
风	微风
	大风
雪	



Growth of Cloud Droplets in a Turbulent Environment



Cloud: A visible aggregate of small water droplets and/or ice particles ($d_p \sim 20 \mu\text{m}$)

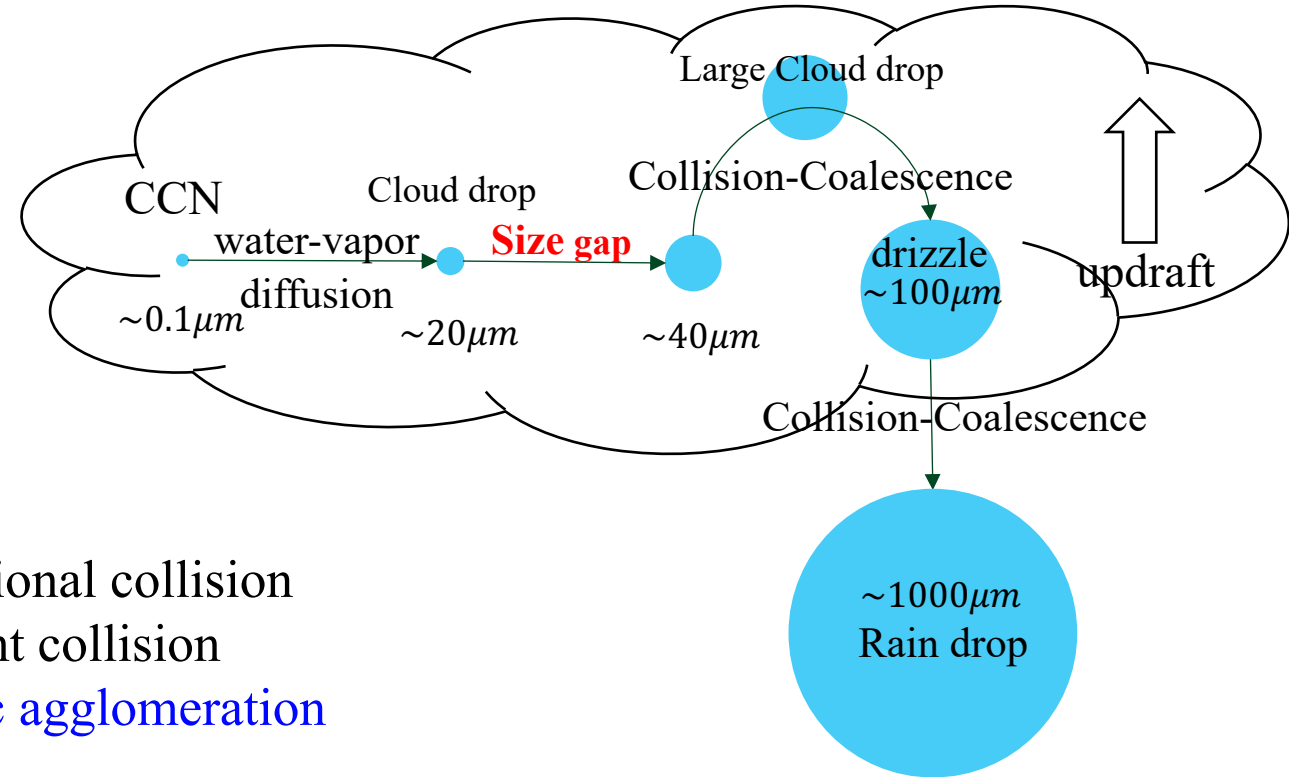
Fog: A cloud very close to the earth's surface.

CCN: Cloud Condensation Nuclei.

Size gap: Size range of $20 - 40 \mu\text{m}$ (neither the diffusional growth nor gravitational collision is effective to increase the droplet size)

Processes for Cloud Droplet Growth:

- **Condensation**
 - **Collision/coalescence**
 - **Ice-crystal process**
-
- Gravitational collision
 - Turbulent collision
 - **Acoustic agglomeration**
 - ...



Our research question: Can we introduce acoustic agglomeration to enhance droplet growth across the size gap?



Specific research objectives

- Develop an improved numerical method to solve SCE
- Study how acoustic agglomeration affects the growth of droplets and drizzle / rain formation
- Use hybrid DNS code to study the collision kernels under the combined action of gravity, acoustic waves, and turbulence



Part 4

An accurate and efficient algorithm for solving
the population balance equation



Description of particle growth due to collision/coalescence

- Population Balance Equation (PBE), Smoluchowski equation, Stochastic Collection Equation (SCE)

$$\frac{\partial n(m, t)}{\partial t} = \underbrace{\int_0^{m/2} n(m - m', t) n(m', t) K(m', m - m') dm'}_{\text{gain term}} - \underbrace{\int_0^\infty n(m, t) n(m', t) K(m, m') dm'}_{\text{loss term}}$$

- Lagrangian particle-based method

Correspond to different numerical schemes:

[Population Balance \(PB\) modeling](#), which is on the macroscopic level.

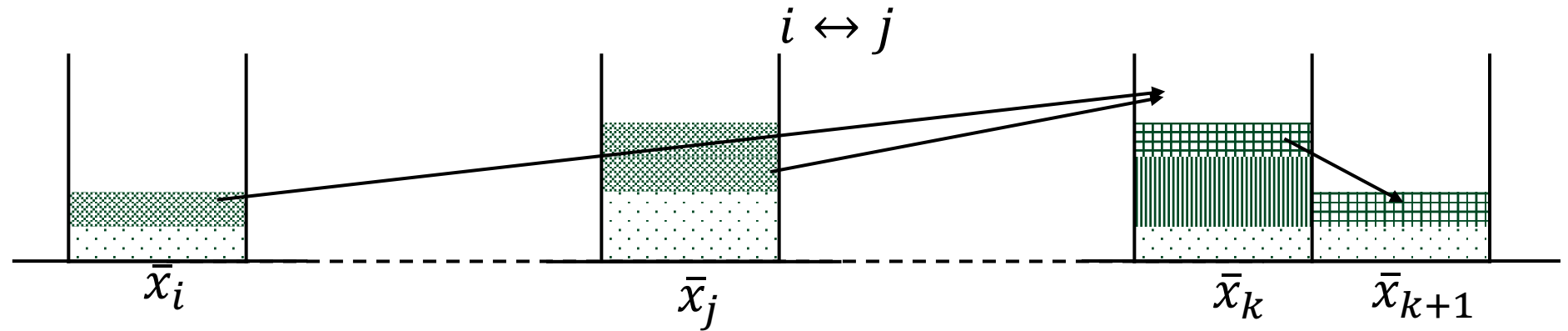
[Lagrangian particle-based numerical simulation approach](#), on the microscopic level.

Numerical methods for solving SCE

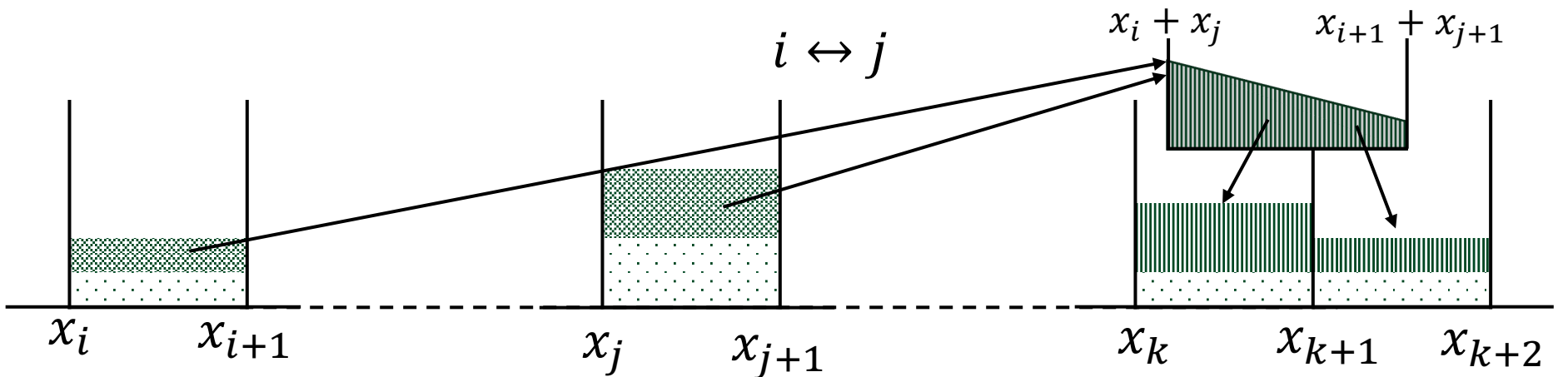


Different numerical methods for solving Stochastic Collection Equation(SCE) have emerged:
 Point-based methods; Spectral moment methods; **Bin-based pair-interaction methods**

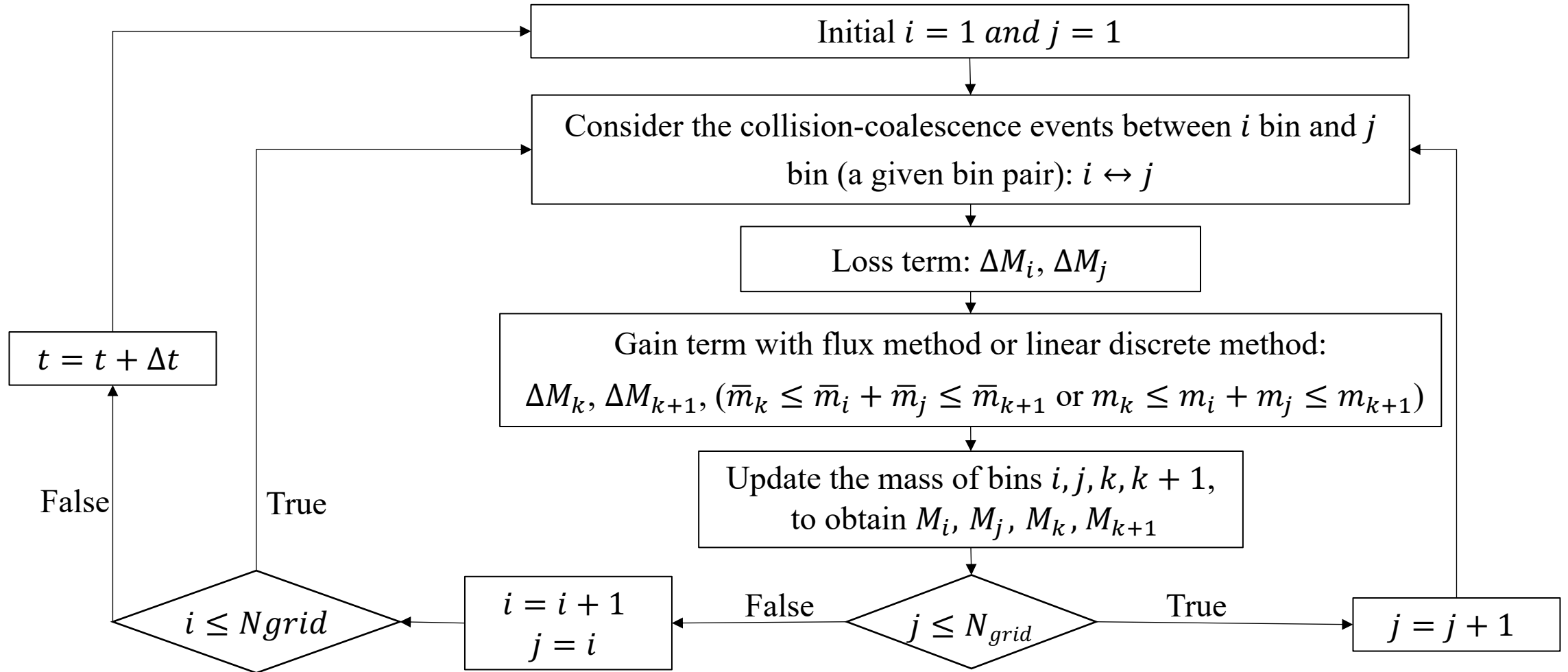
Upstream Flux
 Method
 (UFM)
 $M(x_i, t)$
 [Bott, 1998]



Linear Discrete
 Method
 (LDM)
 $N(x_i, t), M(x_i, t)$
 [Simmel, 2002]



Numerical methods for solving SCE





Issues in the numerical solutions of SCE


- The time derivative is solved using a first-order linear scheme.
- Negative value may appear when calculating the loss integrals.
- Conserving, Positive-Definite, and Unconditionally Stable Scheme is necessary.

$i \leftrightarrow j$: The collision-coalescence events with i and j bins as source bins.

Assume only $i \leftrightarrow j$ occur, for Upstream Flux Method(UFM), we have

$$\frac{\partial g(y_i, t)}{\partial t} = - \int_{y_{j-1/2}}^{y_{j+1/2}} \frac{1}{m_j} g(y_i, t) g(y_j, t) K(y_i, y_j) dy_j \approx - \frac{1}{m_j} g(y_i, t) g(y_j, t) K(y_i, y_j) dy$$

And
$$\frac{\partial g(y_j, t)}{\partial t} \approx - \frac{1}{m_i} g(y_j, t) g(y_i, t) K(y_j, y_i) dy$$


$$\frac{\partial g(y_j, t)}{\partial t} = \frac{\partial g(y_i, t)}{\partial t} \frac{m_j}{m_i} = \frac{\partial g(y_i, t)}{\partial t} Z_{i,j}$$



Analytical pair-wise time integration method + UFM

Suppose $g(y_i, t)$ is continuous and differentiable, we have

$$\begin{aligned}g(y_j, t_n + dt) &= g(y_j, t_n) + \int_{t_n}^{t_n+dt} \frac{\partial g(y_j, t')}{\partial t} dt' = g(y_j, t_n) + \int_{t_n}^{t_n+dt} \frac{\partial g(y_i, t')}{\partial t} \frac{m_j}{m_i} dt' \\ &= g(y_j, t_n) + \frac{m_j}{m_i} \int_{t_n}^{t_n+dt} \frac{\partial g(y_i, t')}{\partial t} dt' = g(y_j, t_n) + \frac{m_j}{m_i} [g(y_i, t_n + dt) - g(y_i, t_n)]\end{aligned}$$

Then



$$\begin{aligned}\frac{\partial g(y_i, t_n + dt)}{\partial t} &= -\frac{1}{m_j} g(y_i, t_n + dt) \left\{ g_j + \frac{m_j}{m_i} [g(y_i, t_n + dt) - g_i] \right\} K(y_i, y_j) dy \\ &= -\frac{K(y_i, y_j) dy}{m_i} g(y_i, t_n + dt)^2 - K(y_i, y_j) dy \left(\frac{g(y_j, t_n)}{m_j} - \frac{g(y_i, t_n)}{m_i} \right) g(y_i, t_n + dt)\end{aligned}$$

$$\text{initial: } g(y_i, t = t_n) = g(y_i, t_n)$$

This is **Bernoulli's differential equation**: $y' + P(x)y = Q(x)y^n, n = 2, 3, \dots$, which have an analytic solution.



Analytical pair-wise time integration method: details

For the sake of simplicity: $g(y_i, t_n) = g_i$ and $g(y_j, t_n) = g_j$. The solution is

$$g(y_i, t_n + dt) = g_i \frac{g_j m_i - g_i m_j}{g_j m_i \exp\left(\left(\frac{g_j}{m_j} - \frac{g_i}{m_i}\right) K(y_i, y_j) dy dt\right) - g_i m_j}, \quad g_j m_i - g_i m_j \neq 0$$

$$g(y_i, t_n + dt) = \frac{m_i g_i}{g_i K(y_i, y_i) dy dt + m_i}, \quad g_j m_i - g_i m_j = 0$$

Gain term can be handled by the flux method (Detail in Bott, 1998), such as upstream flux method (UFM) or linear flux method(LFM).

Then,

$$\sum_{i=1}^M \sum_{j=i}^M i \leftrightarrow j$$

All collision-coalescence events can be accounted

We obtain a Mass Conserving, Positive-Definite, and Unconditionally Stable Scheme

Golovin Kernel



$$K_{i,j} = K(i, j) = b(x_i + x_j) \quad b = 1.5 \text{ m}^3 \text{ kg}^{-1} \text{ s}^{-1}$$

With initial condition

$$n(x, t = 0) = \frac{L}{\bar{x}^2} \exp\left(-\frac{x}{\bar{x}}\right)$$

$$L = 0.001 \text{ kg m}^{-3}, \quad \bar{x} = 4/3 \pi \rho_l \bar{r}^3, \quad \bar{r} = 9.3 \mu\text{m}$$

The analytical solution

$$n(x, t) = \frac{n(v, t)}{\rho_l} = \frac{L}{\bar{x}^2} \phi(x, T) = \frac{L}{\bar{x}^2} \frac{(1-\tau)e^{-x(\tau+1)}}{\pi\tau^{1/2}} I_1(2x\tau^{1/2})$$

$$T = bLt, \quad \tau = 1 - e^{-T}$$

$$I_n(z) = \left(\frac{z}{2}\right)^n \sum_{k=0}^{\infty} \frac{(z^2/4)^k}{k! \Gamma(n+k+1)}, \quad \Gamma(z) = \int_0^{\infty} t^{z-1} e^{-t} dt$$

Numerical Result of Golovin Kernel

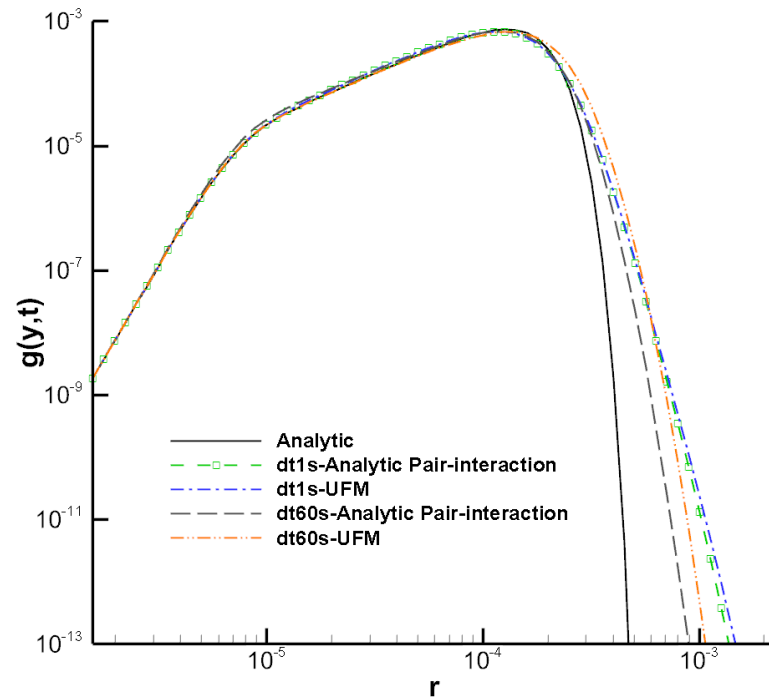


Mass grad

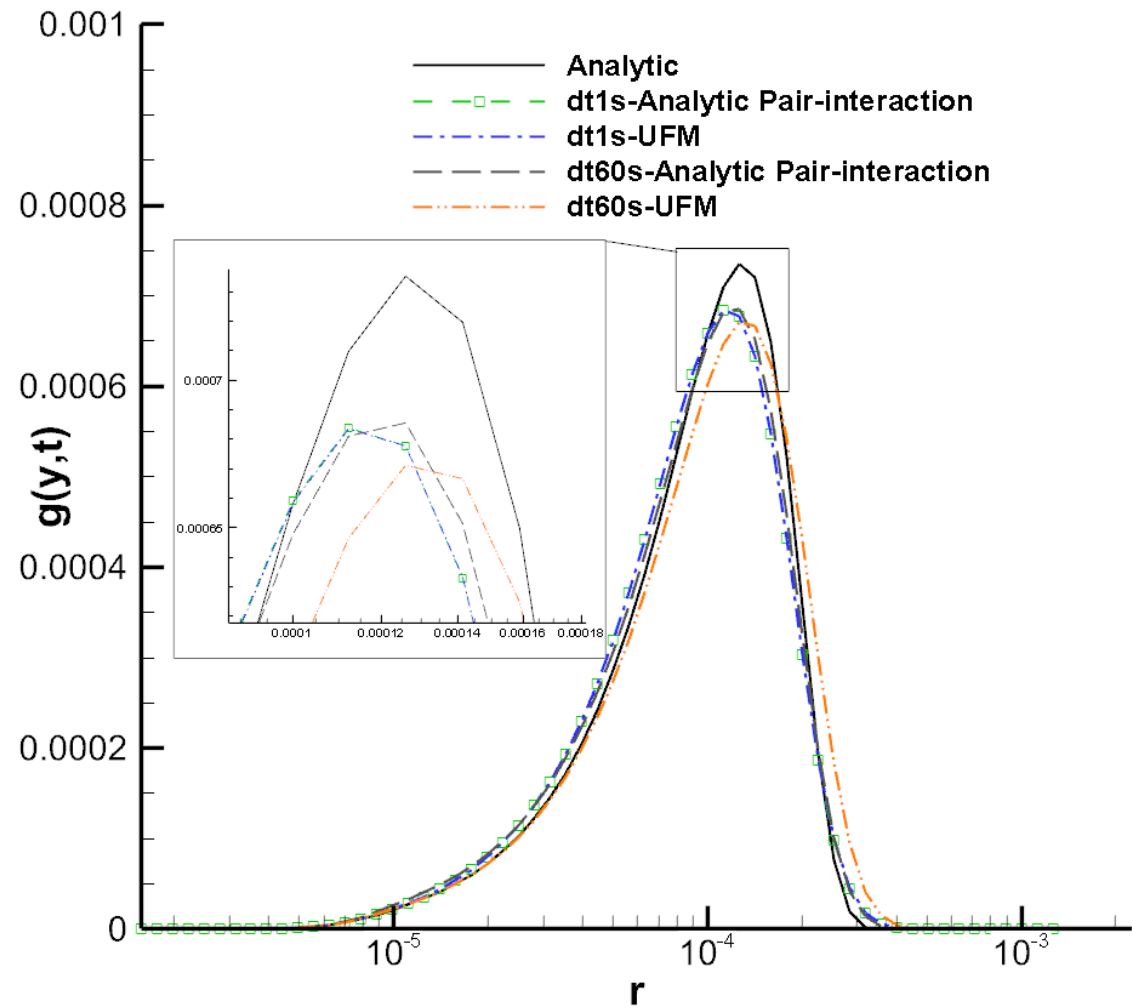
$$m_{i+1} = 2^{1/s} m_i, s = 2$$

We have

$$g(y,t) = 3x^2 n(x,t)$$



$t = 2400s$

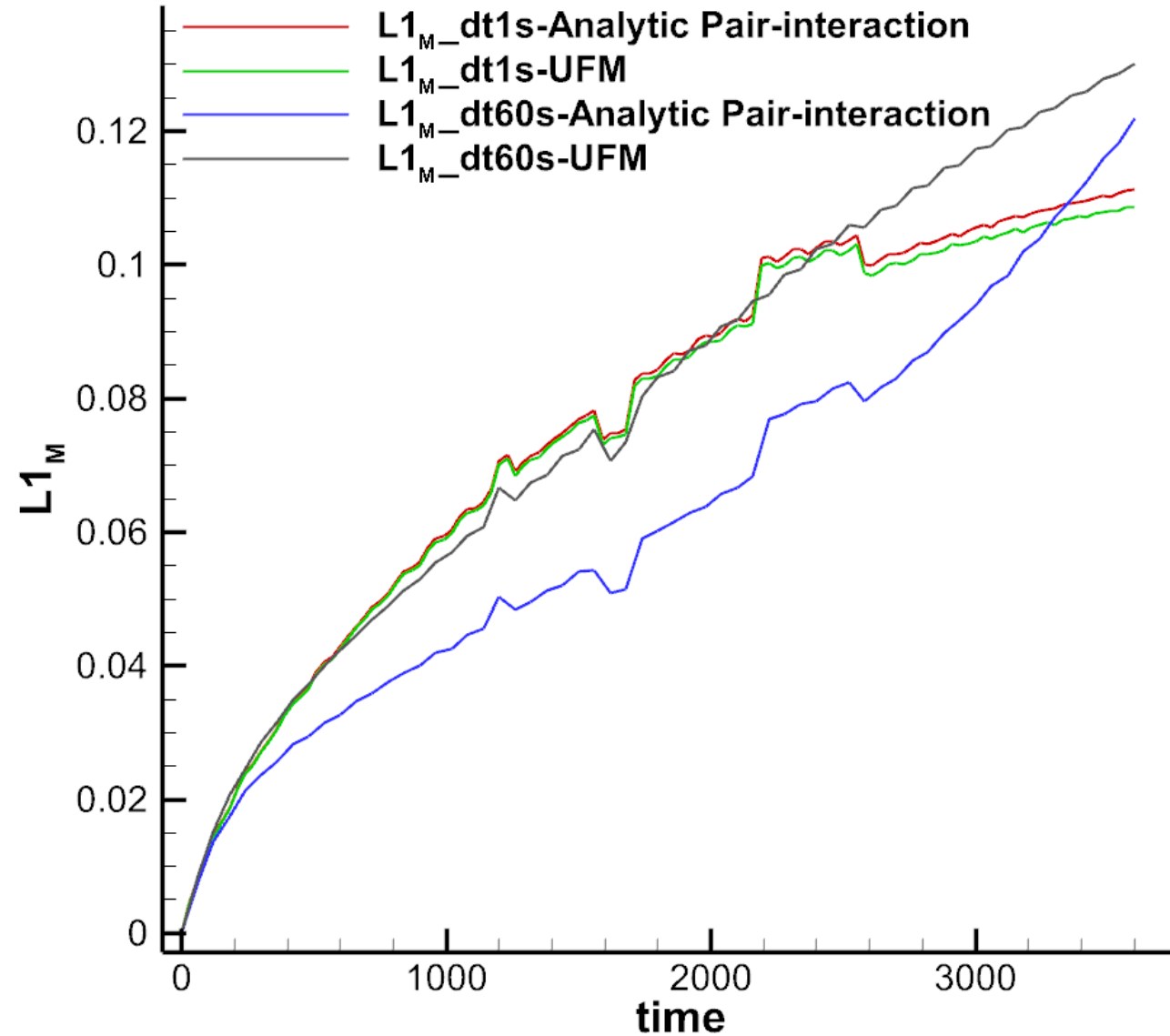


Numerical Result of Golovin Kernel



L1 error for droplet number and mass is

$$L_{1,M} = \frac{1}{L} \sum_i^{N_{grid}} |\hat{M}_i - M_i|$$





Analytical pair-wise time integration method + LDM

The appeal idea can also be applied with Simmel's Linear Discrete Method(LDM)

For $i \leftrightarrow j$

$$\frac{\partial M^0(i, t; i \leftrightarrow j)}{\partial t} = \frac{\partial N(i, t; i \leftrightarrow j)}{\partial t} \approx -K_{i,j} N(i, t; i \leftrightarrow j) N_j(j, t; i \leftrightarrow j)$$

$$\frac{\partial M^0(j, t; i \leftrightarrow j)}{\partial t} = \frac{\partial N(j, t; i \leftrightarrow j)}{\partial t} \approx -K_{i,j} N(i, t; i \leftrightarrow j) N_j(j, t; i \leftrightarrow j)$$

$$\frac{\partial M^1(i, t; i \leftrightarrow j)}{\partial t} = \frac{\partial M(i, t; i \leftrightarrow j)}{\partial t} \approx -K_{i,j} M(i, t; i \leftrightarrow j) N(j, t; i \leftrightarrow j)$$

$$\frac{\partial M^1(j, t; i \leftrightarrow j)}{\partial t} = \frac{\partial M(j, t; i \leftrightarrow j)}{\partial t} \approx -K_{i,j} N(i, t; i \leftrightarrow j) M(j, t; i \leftrightarrow j)$$

For simplicity of writing, omit $i \leftrightarrow j$



Analytical pair-wise time integration method + LDM

We have

$$\frac{\partial N(j,t)}{\partial t} = \frac{\partial N(i,t)}{\partial t}$$

$$\begin{aligned} N(j, t_n + dt) &= N(j, t_n) + \int_{t_n}^{t_n+dt} \frac{\partial N(j, t')}{\partial t} dt' = N(j, t_n) + \int_{t_n}^{t_n+dt} \frac{\partial N(i, t')}{\partial t} dt' \\ &= N(j, t_n) + [N(i, t_n + dt) - N(i, t_n)] \end{aligned}$$

It's physical, and then

$$\begin{aligned} \frac{\partial N(i, t_n + dt)}{\partial t} &\approx -K_{i,j} N(i, t_n + dt) (N(j, t_n) + [N(i, t_n + dt) - N(i, t_n)]) \\ &= K_{i,j} [N(i, t_n) - N(j, t_n)] N(i, t_n + dt) - K_{i,j} N(i, t_n + dt)^2 \end{aligned}$$

$$\text{initial: } N(i, t = t_n) = N(i, t_n)$$

This is **Bernoulli's differential equation**, which have an analytic solution.

$$\frac{dy}{dt} + p(t)y = g(t)y^\alpha$$



Analytical pair-wise time integration method + LDM

The solution is

$$N(i, t) = \frac{N(i, t_n) [N(j, t_n) - N(i, t_n)]}{N(j, t_n) \exp(K_{i,j} [N(j, t_n) - N(i, t_n)] (t - t_n)) - N(i, t_n)} = N(i, t_n) \cdot \Lambda(i, j), \quad N(i, t_n) \neq N(j, t_n)$$

$$N(i, t) \approx \frac{N(i, t_n)}{N(i, t_n) K_{i,j} (t - t_n) + 1}, \quad i = j \text{ or } N(i, t_n) = N(j, t_n)$$

For $M(i, t; i \leftrightarrow j)$, use the appellate relationship, we have

$$\begin{aligned} \frac{\partial M(j, t; i \leftrightarrow j)}{\partial t} &\approx -K_{i,j} N(i, t; i \leftrightarrow j) M(j, t; i \leftrightarrow j) \\ &= -K_{i,j} M(j, t; i \leftrightarrow j) \frac{N(i, t_n) [N(j, t_n) - N(i, t_n)]}{N(j, t_n) \exp(K_{i,j} [N(j, t_n) - N(i, t_n)] (t - t_n)) - N(i, t_n)} \end{aligned}$$

$$\text{initial: } M(i, t = t_n) = M(i, t_n)$$

This equation also has analytical solutions



Analytical pair-wise time integration method + LDM

Finally, For $i \leftrightarrow j$, we get

$$N(i, t_n + dt) \approx N(i, t_n) \cdot \Lambda(i, j)$$

$$N(j, t_n + dt) \approx N(j, t_n) \cdot \Lambda(j, i)$$

$$M(i, t_n + dt) \approx M(i, t_n) \cdot \Lambda(i, j)$$

$$M(j, t_n + dt) \approx M(j, t_n) \cdot \Lambda(j, i)$$

Where

$$\Lambda(i, j) = \begin{cases} \frac{N(i, t_n) [N(j, t_n) - N(i, t_n)]}{N(j, t_n) \exp(K_{i,j} [N(j, t_n) - N(i, t_n)] dt) - N(i, t_n)} & , N(i, t_n) \neq N(j, t_n) \\ \frac{1}{1 + K_{i,j} N(i, t_n) dt} & , N(i, t_n) = N(j, t_n) \end{cases}$$

Then, all collision-coalescence events can be accounted

$$\sum_{i=1}^M \sum_{j=i}^M i \leftrightarrow j$$

Numerical results for the Golovin kernel

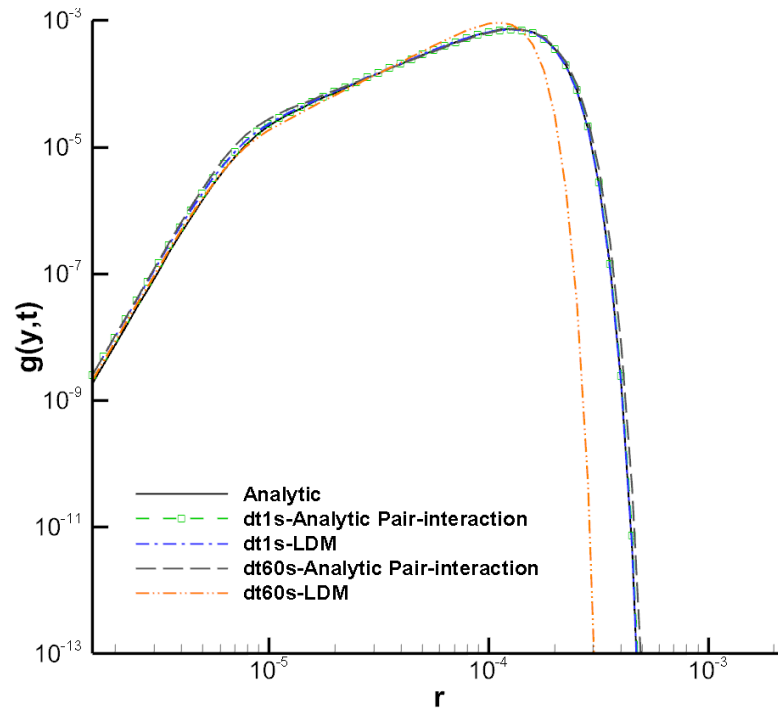


Mass grad

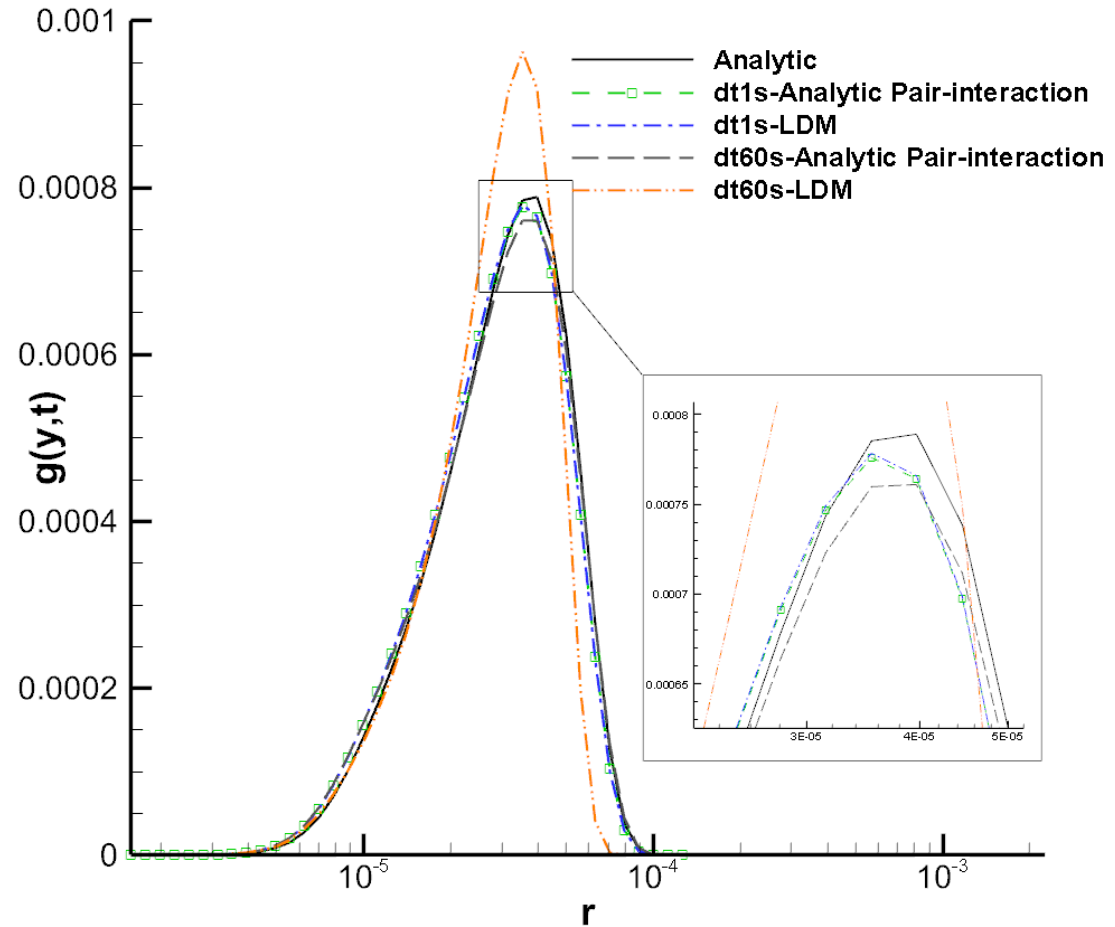
$$m_{i+1} = 2^{1/s} m_i, s = 2$$

We have

$$g(y,t) = 3x^2 n(x,t)$$



$t = 1200s$

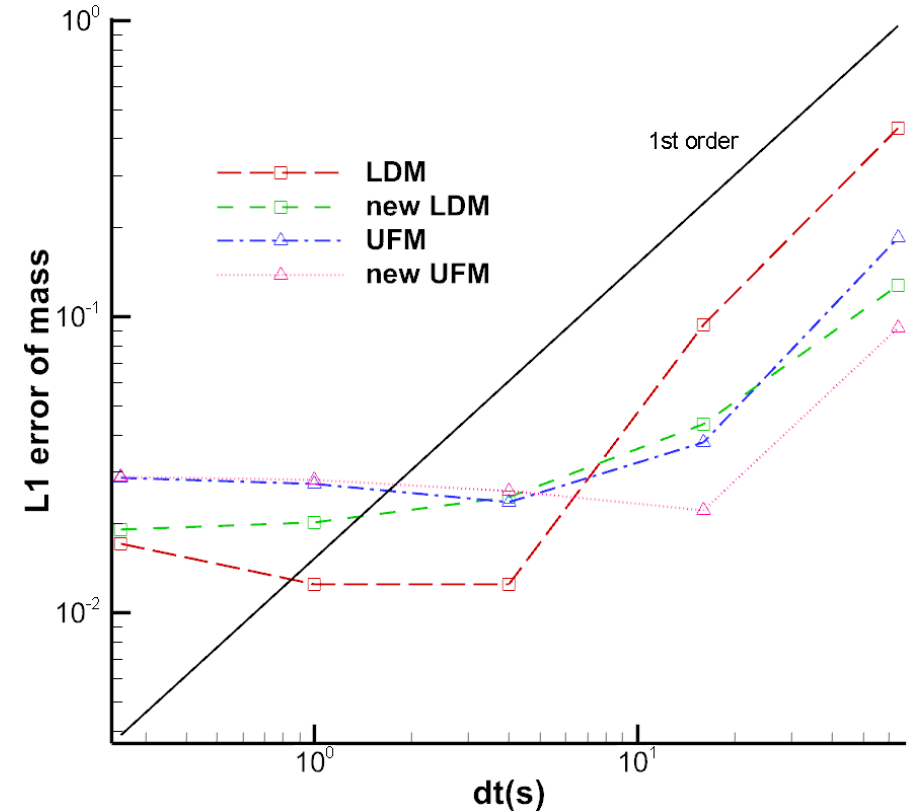
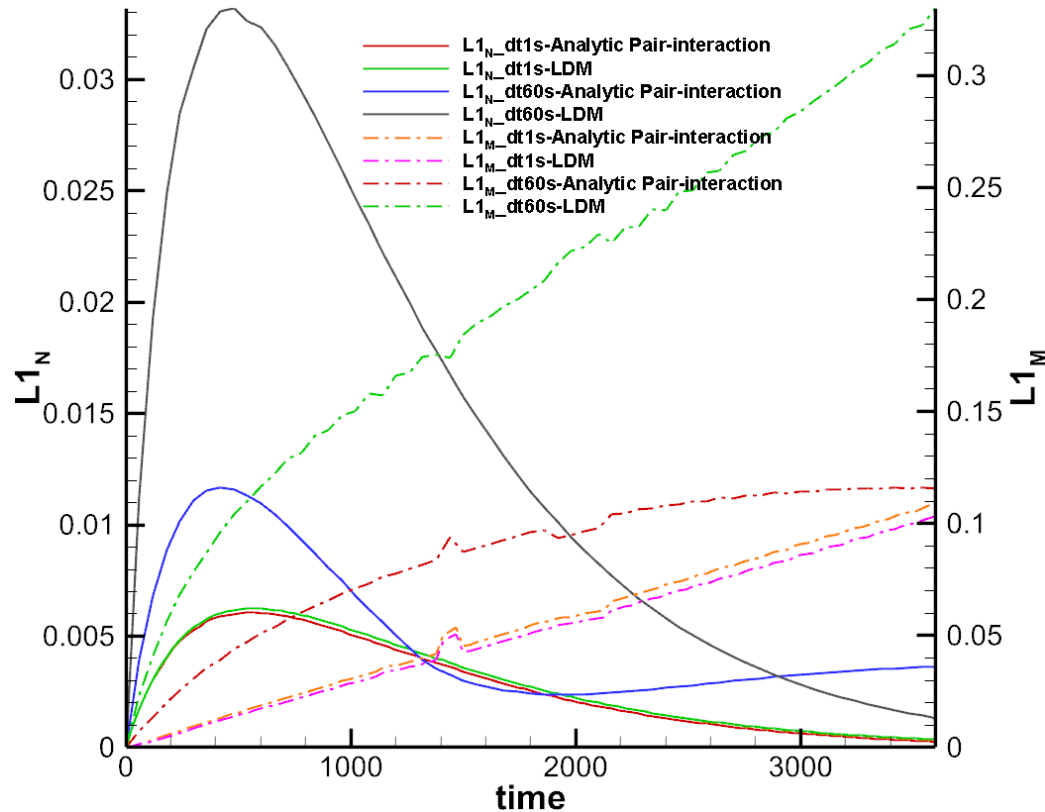


Numerical results for the Golovin Kernel



L1 error for droplet number and mass is

$$L1_N = \frac{1}{N_0} \sum_i^{N_{grid}} |\hat{N}_i - N_i| \quad L1_M = \frac{1}{L} \sum_i^{N_{grid}} |\hat{M}_i - M_i|$$





Summary and conclusions – Part 4

- By treating the collision-coalescence loss outcomes for each bin pair analytically in sequence, we create a conserving, positive-definite, and efficient scheme for solving stochastic collection equation(SCE).
- The proposed treatment can be applied to many traditional schemes of the gain outcome treatments, such as flux method (FM) and Linear Discrete Method (LDM).
- The improved scheme is comparable to the original explicit scheme in efficiency, but has better stability and accuracy when the time step is large.



Part 5

A simple study of effect of sound waves on growth of cloud droplets

Collision kernel due to orthokinetic particle interaction



We set the collision kernel of Orthokinetic is

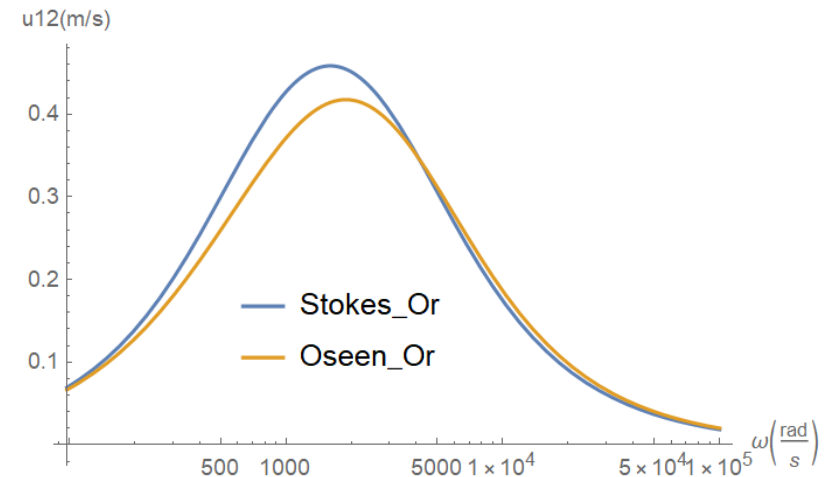
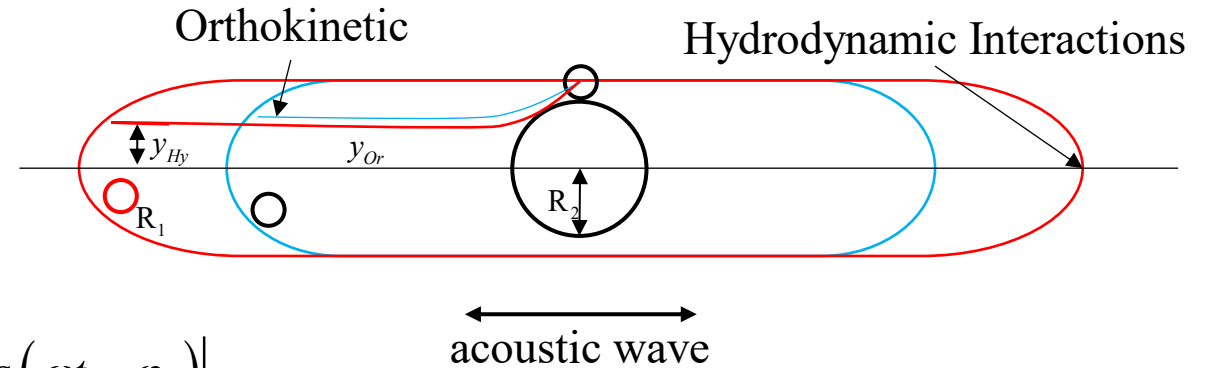
$$K_{ij}^{Or} = \varepsilon_{refill} \varepsilon_{Or} \pi (a_1 + a_2)^2 \bar{u}_{ij}$$

Where

$$\begin{aligned} u_{ij} &= |u_{p,i} - u_{p,j}| = u_0 \left| \sin \varphi_i \cos(\omega t - \varphi_i) - \sin \varphi_j \cos(\omega t - \varphi_j) \right| \\ &= \frac{u_0 \omega |\tau_i - \tau_j|}{\sqrt{1 + (\omega \tau_i)^2} \sqrt{1 + (\omega \tau_j)^2}} \left| \cos(\omega t - \varphi_i - \varphi_j) \right| = \mu_{ij} u_0 \left| \cos(\omega t - \varphi_i - \varphi_j) \right| \end{aligned}$$

$$\bar{u}_{ij} = \mu_{ij} u_0 \frac{2}{\pi}$$

And ε_{refill} is the refilling factor, ε_{Or} is the collision efficient of Orthokinetic interaction.



Collision kernel due to the acoustic wake effect



Assuming the mean distance between the droplet pairs is

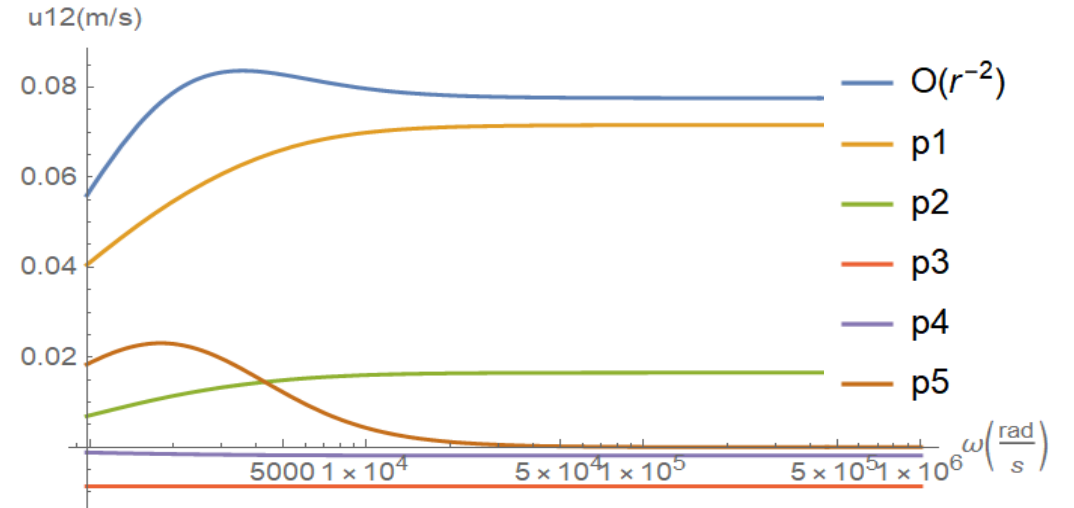
$$r_0 = N^{-1/3}, \quad N \text{ is number concentration}$$

We set the collision kernel of hydrodynamic interactions is

$$K_{ij}^{Hy} = \varepsilon_{refill} \varepsilon_{Hy} \pi (R_1 + R_2)^2 \bar{u}_{ij}$$

$$\approx \varepsilon_{refill} \varepsilon_{Hy} \pi (R_1 + R_2)^2 \left\{ \bar{u}_{12}^{Hy} \approx \underbrace{\frac{3u_0}{2\pi r_0} (R_2 l_2 + R_1 l_1)}_{P1} + \underbrace{\frac{3u_0}{2\pi r_0} \frac{u_0}{\pi \nu} \left((R_2 l_2)^2 + (R_1 l_1)^2 \right)}_{P2} \right.$$

$$\left. - \underbrace{\frac{1}{\pi r_0^2} \frac{6\nu}{\pi} (R_2 + R_1)}_{P3} - \underbrace{\frac{1}{\pi r_0^2} \frac{9u_0}{16} (R_2^2 l_2 + R_1^2 l_1)}_{P4} - \underbrace{\frac{3u_0^2}{8r_0^2 \omega} l_1 l_2 (l_1 q_2 - q_1 l_2) (R_2 - R_1)}_{P5} \right\}$$



The combined kernel



Assume

$$K_{ij} = K_{G,ij} + K_{Hy,ij} + K_{Or,ij}$$
$$= E_{G,coal} \left(\varepsilon_G \pi (R_1 + R_2)^2 |u_i - u_j| + \varepsilon_{Hy,refill} \varepsilon_{Hy} \pi (R_1 + R_2)^2 \bar{u}_{Hy,ij} + \varepsilon_{Or,refill} \varepsilon_{Or} \pi (R_1 + R_2)^2 \bar{u}_{Or,ij} \right)$$

$$\varepsilon_{Hy,refill} \varepsilon_{Hy} = \varepsilon_{Or,refill} \varepsilon_{Or} = 1$$

$E_{G,coal}, \varepsilon_G$ Deal with Onishi and Takahashi, 2012

Initial distribution

$$n(D, t = 0) = N'_0 D^v \exp(-\lambda D^\mu)$$

Where LWC is initial liquid water content, N_0 is initial number concentration, \bar{D} is the mode size of initial distribution, we have

$$LWC = \frac{\pi \rho_l N_0}{6\lambda} = \frac{\pi \rho_l N_0 \bar{D}^3}{4}, \quad \lambda = \frac{2}{3\bar{D}^3}, \quad N'_0 = 3\lambda N_0$$

Like Liu, 1995, set $v = 2, \mu = 3$



Bin grid convergence

Mass grid

$$m_{i+1} = 2^{1/s} m_i \quad m_0 = 1 \mu m$$

Set

$$s = 2, N_{grid} = 70$$

$$s = 3, N_{grid} = 100$$

$$s = 4, N_{grid} = 120$$

Result

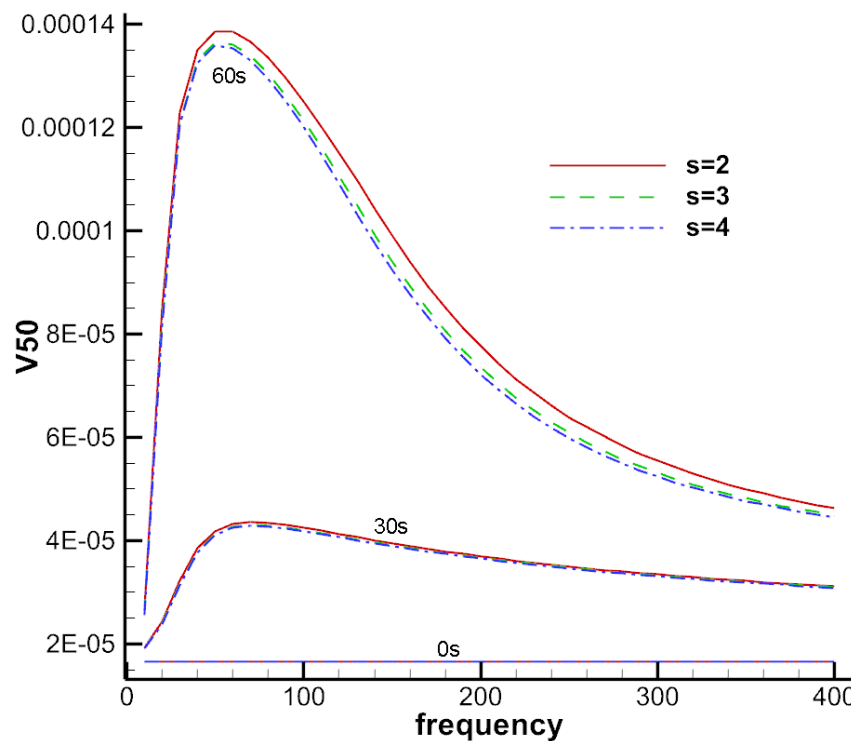
$$LWC = 20 \text{ g cm}^{-3}$$

$$\bar{D} = 12.2 \mu m$$

$$SPL = 130 \text{ dB}$$

$$a = 340 \text{ m s}^{-1}$$

30s, 60s



$$r_{V10} = \frac{V10(t) - V10(t=0)}{V10(t=0)}$$

$$r_{V50} = \frac{V50(t) - V50(t=0)}{V50(t=0)}$$

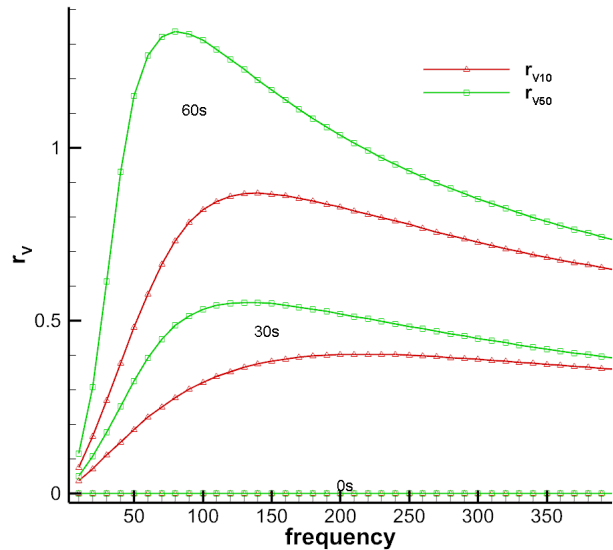
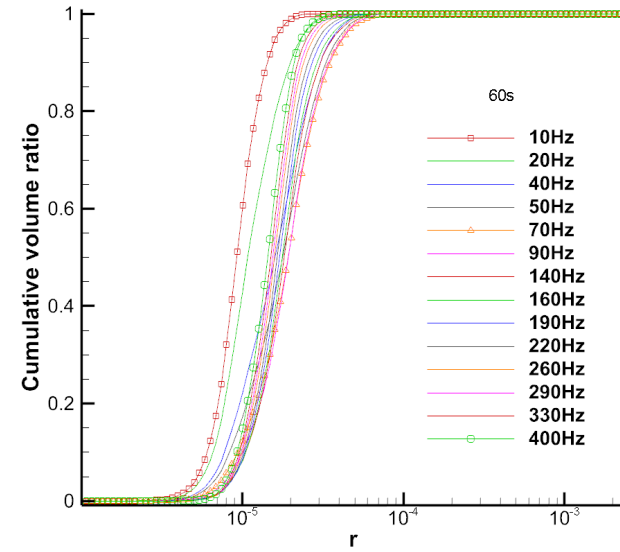
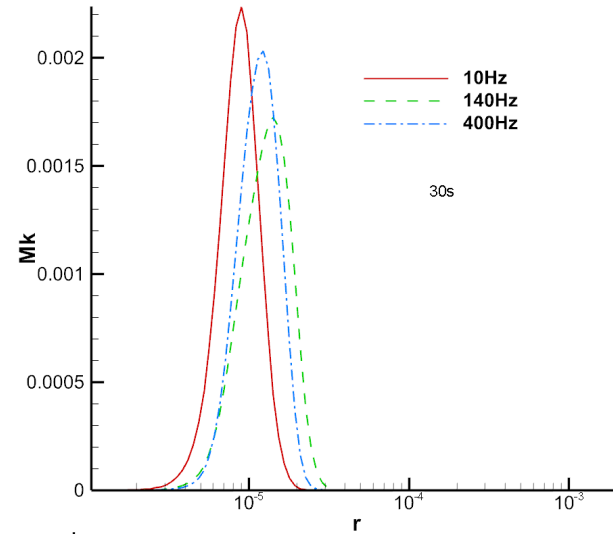
The effect of different kernel choices



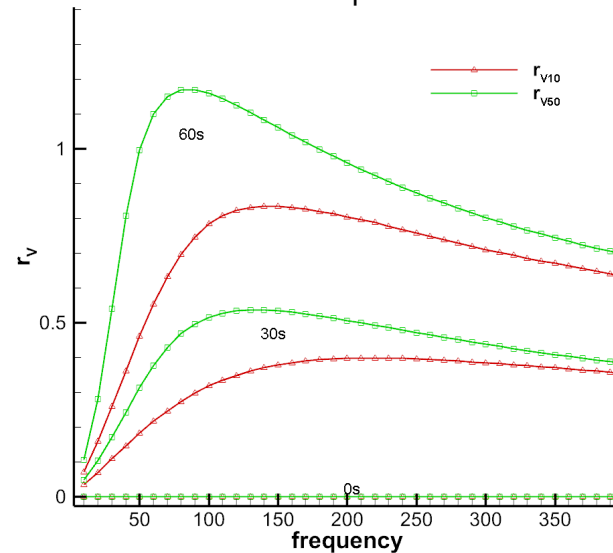
$$LWC = 20 \text{ g cm}^{-3}, \bar{D} = 12.2 \text{ } \mu\text{m}$$

$$SPL = 122 \text{ dB}, a = 340 \text{ m s}^{-1}$$

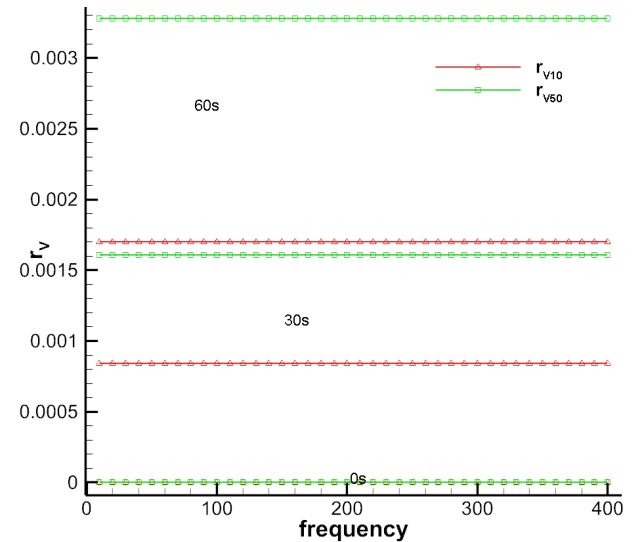
30s, 60s



Gravity kernel+ Acoustic Kernel



Only Acoustic Kernel



Only Gravity kernel

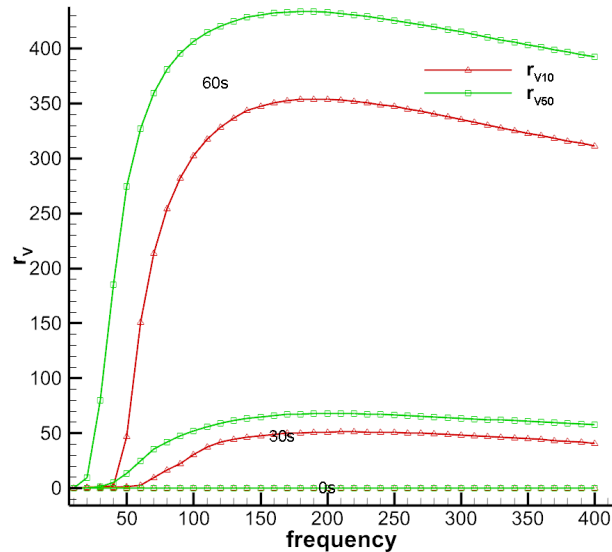
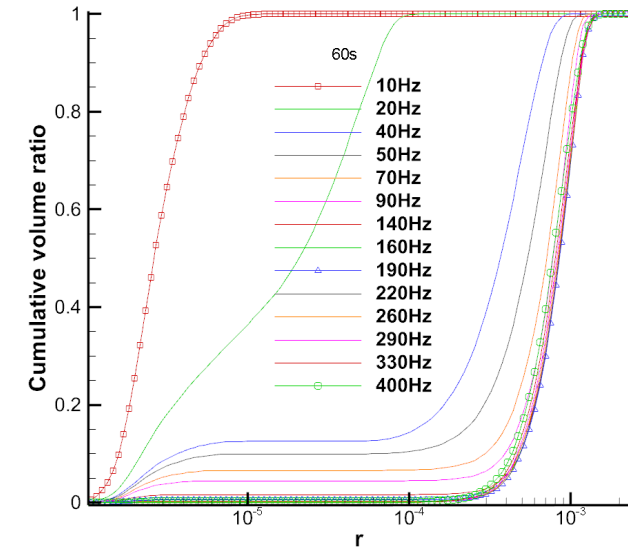
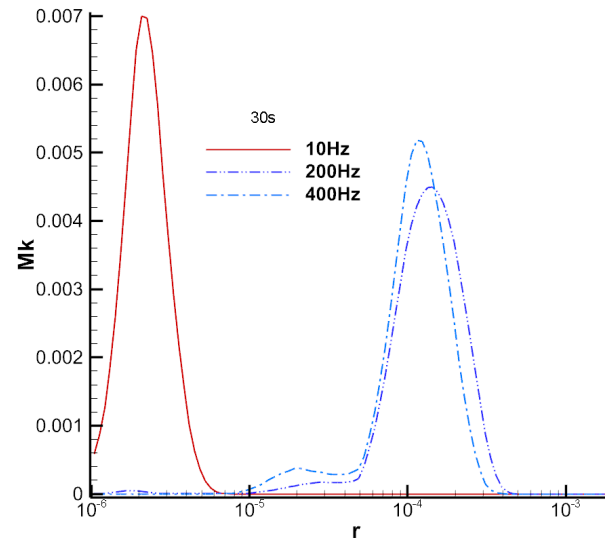
The effect of different kernel choices



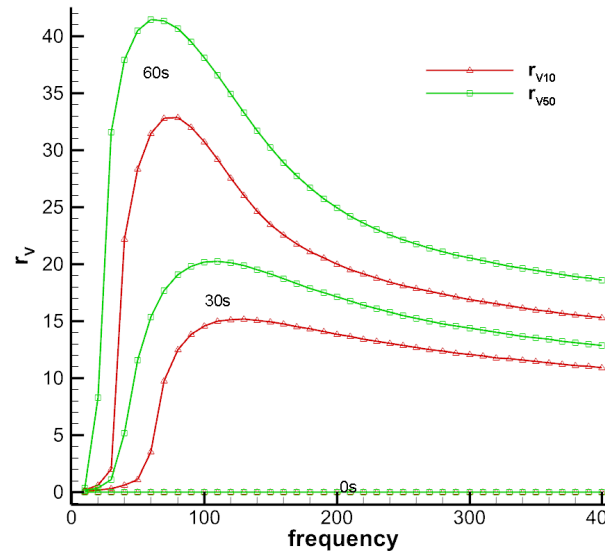
$$LWC = 72.5 \text{ g cm}^{-3}, \bar{D} = 2.87 \text{ } \mu\text{m}$$

$$SPL = 129.8 \text{ dB}, a = 340 \text{ m s}^{-1}$$

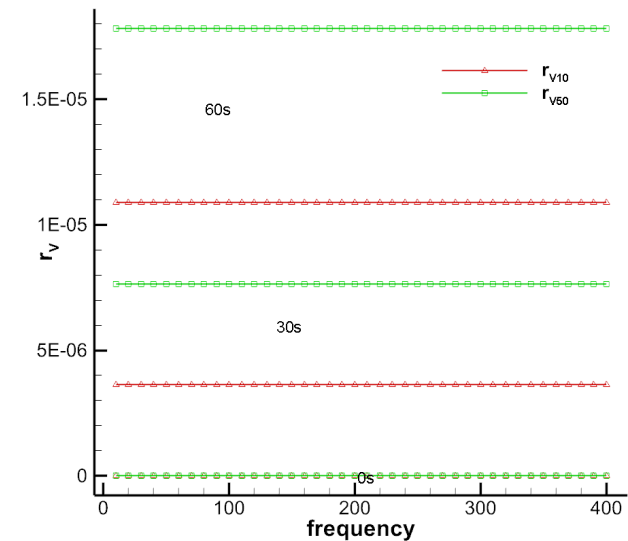
30s, 60s



Gravity kernel+ Acoustic Kernel



Only Acoustic Kernel



Only Gravity kernel

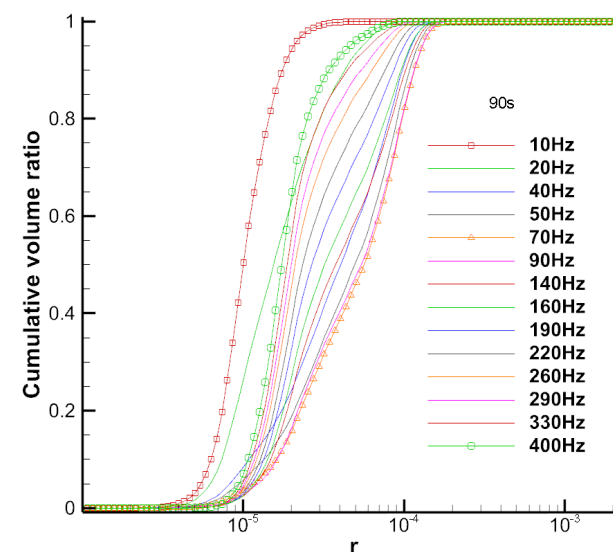
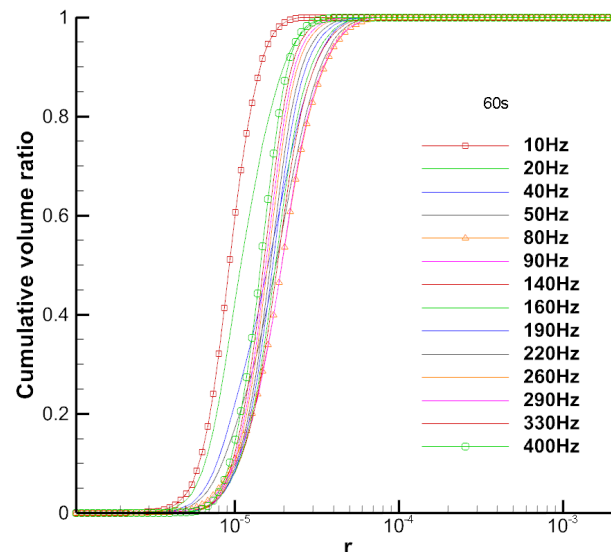
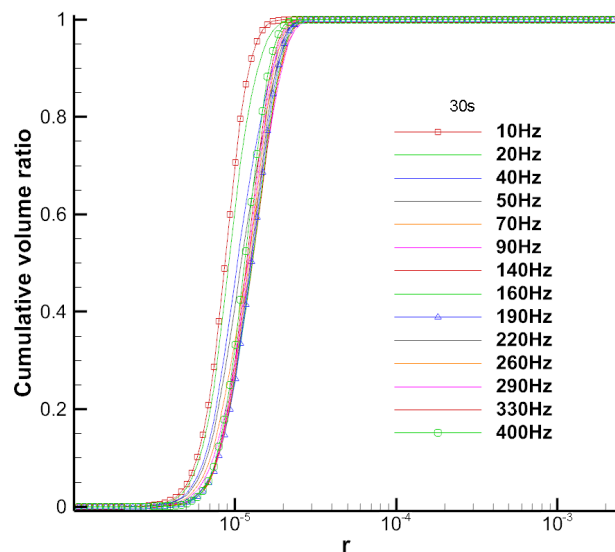
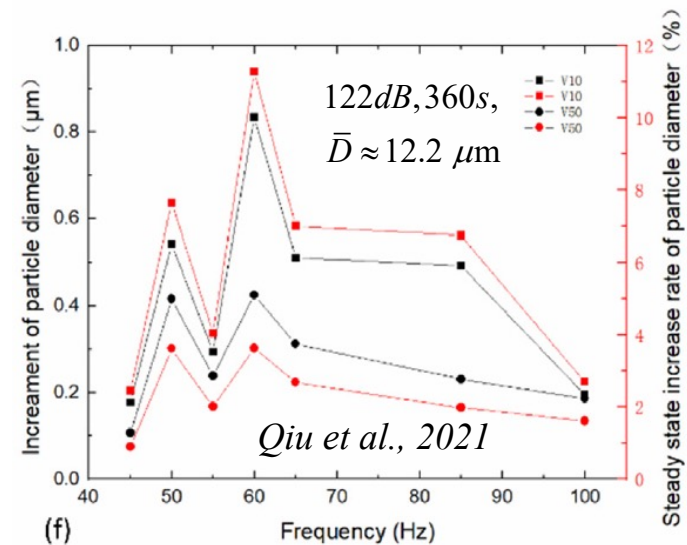
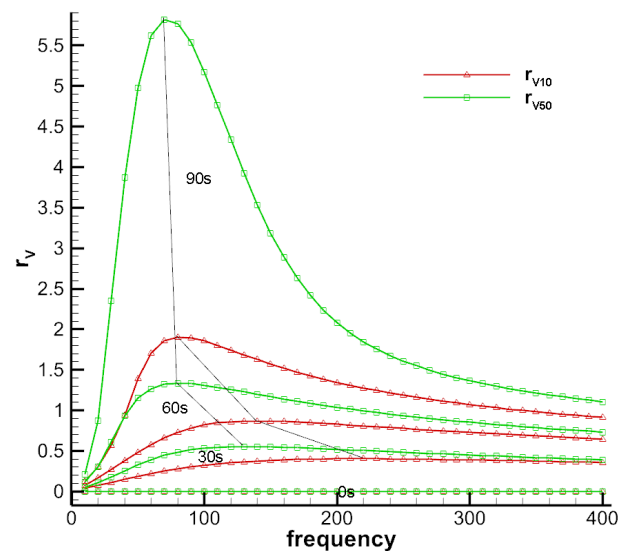


The effect of sound-wave residence time

$$LWC = 20 \text{ g cm}^{-3}, \bar{D} = 12.2 \text{ } \mu\text{m}$$

$$SPL = 122 \text{ dB}, a = 340 \text{ m s}^{-1}$$

30s, 60s, 90s



The effect of sound pressure level



$$LWC = 20 \text{ g cm}^{-3}, \bar{D} = 16 \text{ }\mu\text{m}, a = 340 \text{ m s}^{-1}, 30s$$

<i>SPL dB</i>	80	90	100	110	120	130	140	150
Opti freq, V10	205	200	200	180	150	90	30	20
Ratio V10	0.005412	0.01035	0.02647	0.08203	0.2463	0.8283	3.7417	8.4452
Opti freq, V50	140	140	140	120	100	50	30	20
Ratio V50	0.009142	0.01511	0.03404	0.09614	0.3206	1.3192	5.2771	9.1727

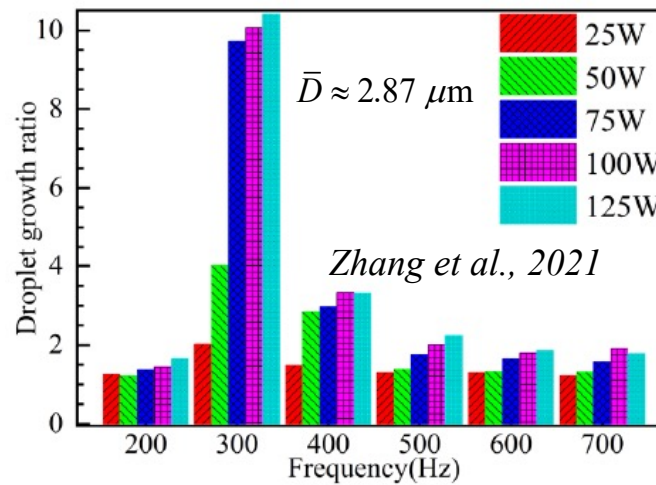
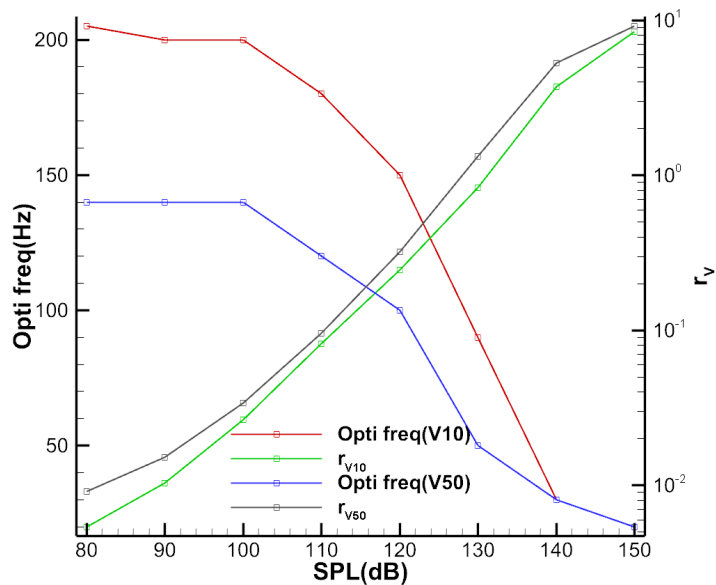
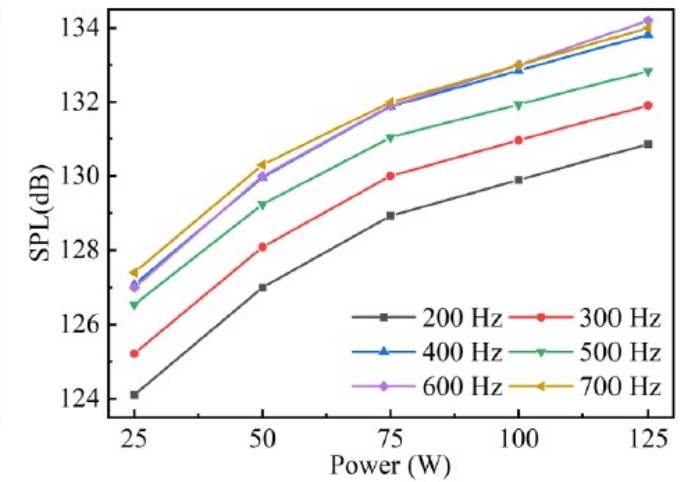


Figure 5. Effect of frequency on droplet growth ratio at applied lasting time of 30 s, initial mass concentration of 72.5 g m^{-3} .





The effect of the initial droplet size distribution

$$SPL = 122 \text{ dB}, a = 340 \text{ m s}^{-1}, 60s$$

$$\bar{D} = 10 \text{ } \mu\text{m}$$

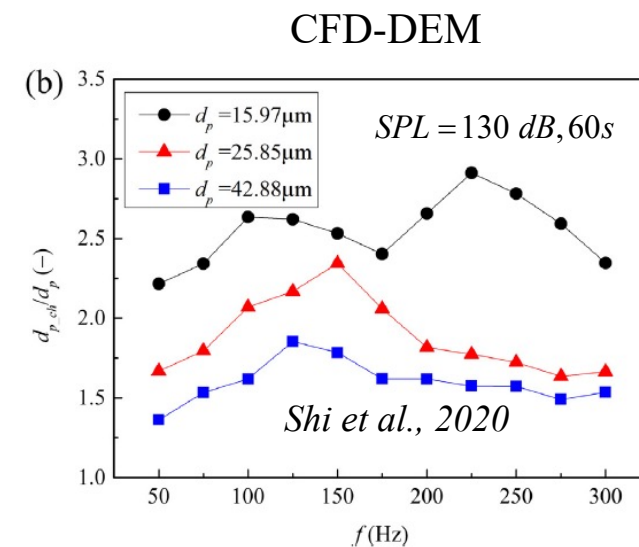
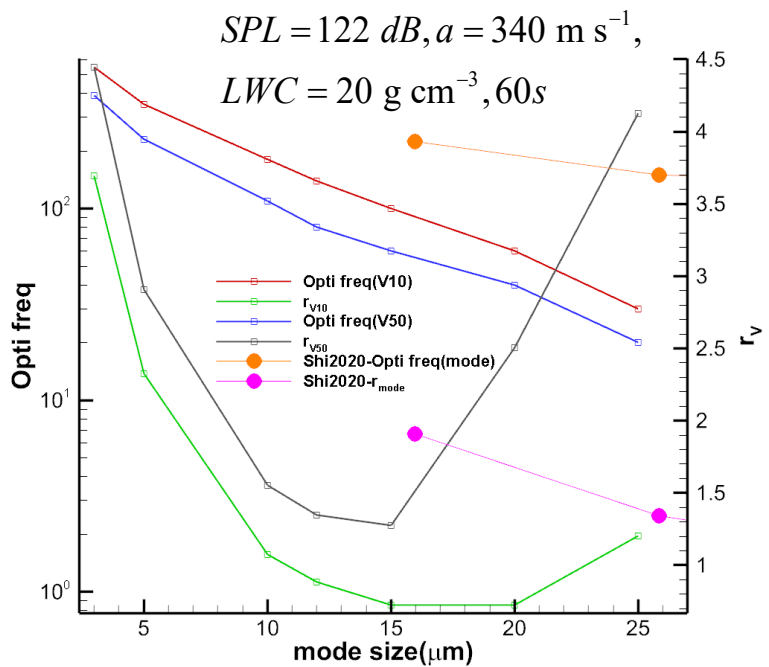
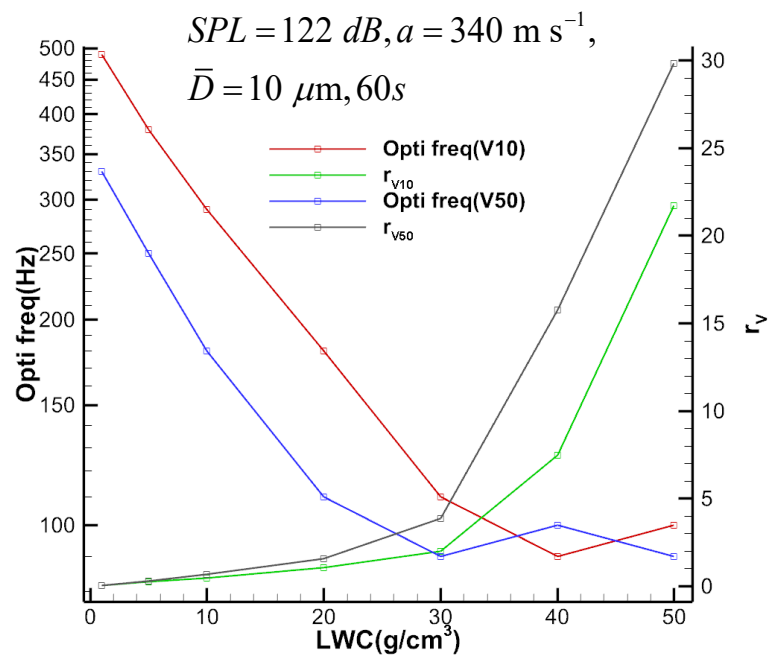
LWC g/cm³	1	5	10	20	30	40	50
Opti freq, V10	490	380	290	180	110	90	100
Ratio V10	0.0466	0.2369	0.4829	1.0726	2.011	7.4595	21.7209
Opti freq, V50	330	250	180	110	90	100	90
Ratio V50	0.0519	0.2948	0.6716	1.5508	3.8827	15.776	29.8365

$$LWC = 20 \text{ g cm}^{-3}$$

\bar{D} μm	3	5	10	12	15	20	25
Opti freq, V10	550	350	180	140	100	60	30
Ratio V10	3.6963	2.3274	1.0726	0.8817	0.7237	0.7243	1.2031
Opti freq, V50	390	230	110	80	60	40	20
Ratio V50	4.4474	2.9065	1.5508	1.3489	1.2748	2.5071	4.1266



The effect of the initial droplet size distribution





The Time and Length Scales of Sound Wave Compared to Turbulence in Clouds

Under the standard atmospheric condition: $T=25\text{ }^{\circ}\text{C}$, $\rho = 1.182\text{ kg} \cdot \text{m}^{-3}$, $c = 343\text{ m/s}$

$$p_{rms} = \frac{\delta p_0}{\sqrt{2}} = \sqrt{I\rho c} = \sqrt{I_0 \times 10^{(SIL/10)} \rho c} = \sqrt{10^{-12} \times 10^{(SIL/10)} \cdot 1.182 \cdot 343} = 2.01 \times 10^{-5} \times 10^{(SIL/20)}$$

For typical turbulence in the atmosphere, we have

$$u_{rms} \sim 1\text{ m/s}, L \sim 100\text{ m}, \varepsilon \sim 0.01\text{ m}^2/\text{s}^3$$

	SIL(dB)	$I(W \cdot m^{-2})$	$p_{rms}(\text{Pa})$	Frequency $f(\text{Hz})$	Length scale(m)	Time Scale (s)
Air turbulence	-	$(p_{rms}u_{rms}) \sim 1$	~ 1	-	$L \sim 100$ $\eta \sim 0.001$	$T \sim \frac{L}{u_{rms}} \sim 100\text{ s}$ $\tau_K \sim 0.04\text{ s}$
Cloud droplets	-	-	-	-	$a_p \sim 10^{-5}$ $a_p \ll \lambda$	$\tau_p \sim 0.001\text{ s}$
sound	0	1×10^{-12}	20×10^{-6}	10	$\lambda \sim 30$	0.1
	80	1×10^{-4}	0.2	100	$\lambda \sim 3$	0.01
	150	1×10^3	636	1000	$\lambda \sim 0.3$	0.001

- (1) The acoustic forcing can cause large pressure fluctuations compared to turbulence fluctuations.
- (2) The acoustic forcing can interact with turbulent fluctuations



Summary and conclusions – Part 5

- Intense sound-wave field can promote relative motion and agglomeration among cloud droplets, and the effect of acoustic agglomeration depends on SPL.
- By numerically solving the stochastic coalescence equation, we investigated the optimal frequency of acoustic agglomeration, in the presence of gravitational and sound-wave induced collision-coalescence, for different initial size distributions of cloud droplets.
- Qualitative result:
 1. Sound waves can promote the growth of small cloud droplets to the size range for which gravitational coagulation becomes effective.
 2. The optimal frequency decreases with the increasing duration of the applied sound wave and the increasing SPL of the sound wave.
 3. The optimal frequency decreases with the increase of the initial liquid water content and the initial mode size, but the effect of acoustic agglomeration is not monotonous with the increase of the initial mode size.